Simulating emission and chemical evolution of coarse sea-salt particles in the Community Multiscale Air Quality (CMAQ) model

J. T. Kelly[1,*], P. V. Bhave[1], C. G. Nolte[1], U. Shankar[2], and K. M. Foley[1]

[1]{Atmospheric Modeling and Analysis Division, National Exposure Research Laboratory, Office of Research and Development, U.S. Environmental Protection Agency, RTP, NC}

[2]{Institute for the Environment, University of North Carolina, Chapel Hill, NC}

[*] {now at: Planning and Technical Support Division, Air Resources Board, California Environmental Protection Agency, Sacramento, CA}

Correspondence to J. T. Kelly (jkelly@arb.ca.gov)

Abstract

Chemical processing of sea-salt particles in coastal environments significantly impacts concentrations of particle components and gas-phase species and has implications for human exposure to particulate matter and nitrogen deposition to sensitive ecosystems. Emission of sea-salt particles from the coastal surf zone is known to be elevated compared to that from the open ocean. Despite the importance of sea-salt emissions and chemical processing, the U.S. EPA's Community Multiscale Air Quality (CMAQ) model has traditionally treated coarse sea-salt particles as chemically inert and has not accounted for enhanced surf-zone emissions. In this article, updates to CMAQ are described that enhance sea-salt emissions from the coastal surf zone and allow dynamic transfer of HNO_3, H_2SO_4, HCl, and NH_3 between coarse particles and the gas phase. Predictions of updated CMAQ models and the previous release version, CMAQv4.6, are evaluated using observations from three coastal sites during the Bay Regional Atmospheric Chemistry Experiment (BRACE) in Tampa, FL in May 2002. Model updates improve predictions of NO_3^-, SO_4^{2-}, NH_4^+, Na^+, and Cl^- concentrations at these sites with only a 8% increase in run time. In particular, the chemically interactive coarse particle mode dramatically

improves predictions of nitrate concentration and size distributions as well as the fraction of total nitrate in the particle phase. Also, the surf-zone emission parameterization improves predictions of total sodium and chloride concentration. Results of a separate study indicate that the model updates reduce the mean absolute error of nitrate predictions at coastal CASTNET and SEARCH sites in the eastern U.S. Although the new model features improve performance relative to CMAQv4.6, some persistent differences exist between observations and predictions. Modeled sodium concentration is biased low and causes under-prediction of coarse particle nitrate. Also, CMAQ over-predicts geometric mean diameter and standard deviation of particle modes at the BRACE sites. These over-predictions may cause too rapid particle dry deposition and partially explain the low bias in sodium predictions. Despite these shortcomings, the updates to CMAQ enable more realistic simulations of chemical processes in environments where marine air mixes with urban pollution. The model updates described in this article are included in the public release of CMAQv4.7 (http://www.cmaq-model.org).

1 Introduction

Sea-salt particles emitted by oceans contribute significantly to the global aerosol burden on a mass basis (Seinfeld and Pandis, 1998; Lewis and Schwartz, 2004). Sea-salt emissions are also important on a number basis and impact concentrations of cloud condensation nuclei (Pierce and Adams, 2006). Upon emission, sea-salt particles have chemical composition similar to their oceanic source (e.g., major ions: Na^+, Mg^{2+}, Ca^{2+}, K^+, Cl^-, SO_4^{2-}; Tang et al., 1997), but they are processed chemically during atmospheric transport. For instance, a number of studies have reported uptake of gaseous acids by sea salt: e.g., nitric acid (Gard et al., 1998 and references therein), sulfuric acid (McInnes et al., 1994), dicarboxylic acids (Sullivan and Prather, 2007), and methylsulfonic acid (Hopkins et al., 2008). Given the large contribution of sea salt to atmospheric particulate matter (PM), the emission and chemical evolution of sea-salt particles must be represented accurately by models.

The diameter of sea-salt particles spans several orders of magnitude, but the peak in the mass distribution is usually in the coarse size range (aerodynamic diameter, D_{aero}, > 2.5 μm) (e.g., Keene et al., 2007). Uptake of gaseous species by coarse sea-salt particles reduces their

availability for condensation on fine particles and can potentially reduce the mass concentration of $PM_{2.5}$ (PM with $D_{aero} \leq 2.5$ μm). Uptake by coarse sea salt can also significantly reduce the concentration of nitric acid in environments where the formation of particulate ammonium nitrate is unfavorable (e.g., ammonia-limited or high-temperature). Associations between coarse particle nitrate and sea salt have been observed in both coastal (e.g., Hsu et al., 2007) and rural (e.g., Lee et al., 2008) areas.

Sea-salt emissions are enhanced in the coastal surf zone compared to the open ocean and result in elevated concentrations near the coast (de Leeuw et al., 2000). During advection toward land, sea salt is often exposed to anthropogenic emissions from shipping lanes (Osthoff et al., 2008; Simon et al., 2009) and coastal urban centers (Nolte et al., 2008). Considering that many coastal areas are densely populated (Nicholls and Small, 2002), chemical modification of sea-salt particles by acidic gases could result in significant human exposure to anthropogenic PM_{10} (PM with $D_{aero} \leq$ 10 μm) in coastal environments. This exposure is a concern in light of associations between increases in coarse particle concentrations and adverse health effects (Brunekreef and Forsberg, 2005; Sandstrom et al., 2005; Volckens et al., 2009).

Despite the significance of sea-salt emissions and chemical transformations, some prominent air quality models have not treated sea-salt particles (e.g., Bessagnet et al., 2004; Grell et al., 2005). Other models have included emissions of sea-salt particles, but have not simulated their chemical interactions with gas-phase species (e.g., Foltescu et al., 2005; Smyth et al., 2009). The U.S. EPA's Community Multiscale Air Quality (CMAQ) model has included online calculation of sea-salt emissions from the open ocean since version 4.5, but has not accounted for enhanced emissions from the coastal surf zone and has treated coarse sea-salt particles as dry and chemically inert (Sarwar and Bhave, 2007).

Studies that have simulated the chemical evolution of sea-salt particles have used alternative models to CMAQ (e.g., Jacobson, 1997; Lurmann et al., 1997; Meng et al., 1998; Sun and Wexler, 1998b; Sartelet et al., 2007; Athanasopoulou et al., 2008; Pryor et al., 2008) or variants of CMAQ such as CMAQ-MADRID (Zhang et al., 2004). These studies often suffered from simple estimates of sea-salt emissions or did not evaluate model results against measurements of size-segregated PM composition (i.e., size-composition distributions). Spyridaki et al. (2006) did evaluate size-composition distributions, but did not account for enhanced emissions of sea salt

from the coastal surf zone. Kleeman and Cass (2001) modeled surf-zone emissions, but only evaluated size-composition distributions for particles with $D_{aero} < 1.8$ μm. A recent example of a CMAQ variant that treats chemical processing of sea salt is CMAQ-UCD (Zhang and Wexler, 2008). This model was developed for application in the Bay Regional Atmospheric Chemistry Experiment (BRACE) (Nolte et al., 2008). Although CMAQ-UCD performed well in that study, the model is not suitable for many applications because its run speed is about 8-10 times slower than the standard version of CMAQ used for regulatory applications. Despite the numerous modeling efforts described above, a need exists for a computationally-efficient treatment of sea-salt emissions and chemical evolution in a model where results capture the size-composition distributions observed in coastal environments.

The BRACE study was conducted to (1) improve estimates of atmospheric nitrogen deposition to Tampa Bay, FL, (2) apportion nitrogen deposition to local and non-local sources, and (3) assess the impact of utility controls on nitrogen deposition to Tampa Bay (Atkeson et al., 2007). Excessive nitrogen addition to waterways from the atmosphere and land can produce eutrophic conditions detrimental for aquatic life (e.g., low dissolved O_2 and high opacity). In 2004, 65% of assessed systems in the continental U.S. had moderate to high eutrophic conditions (Bricker et al., 2007). Due to the different deposition velocities of gases and particles, condensation of HNO_3 and NH_3 on coarse sea salt can alter nitrogen deposition to sensitive ecosystems (Pryor and Sorensen, 2000; Evans et al., 2004). Studies that apportion nitrogen deposition to potentially controllable sources could benefit from models that accurately and efficiently calculate the chemical processing and deposition of sea salt.

Air quality models require good predictions of particle size distributions to accurately predict dry deposition. Accurate size distributions are also important to the ongoing development of an inline photolysis module for CMAQ (Foley et al., 2009) and the coupled meteorology and chemistry model, WRF-CMAQ (Pleim et al., 2008), which calculate the impact of atmospheric particles on radiative transfer and clouds. Lung dosimetry models also require information on particle size, because deposition patterns in the lung depend strongly on particle diameter in addition to flow variables and lung morphometry (Asgharian et al., 2001). Due to the regulatory emphasis on mass-based PM concentrations, particle size distributions from the CMAQ model are rarely evaluated against observations. In cases where they have been evaluated (Elleman and

Covert, 2009; Park et al., 2006; Zhang et al., 2006), the focus has been on number or volume distributions of fine particles. The availability of size-resolved PM composition measurements from the BRACE campaign that span two-orders of magnitude ($0.18 < D_{aero} < 18$ μm) provides an opportunity to evaluate CMAQ predictions of size-composition distributions in a coastal urban environment.

In this study, CMAQ is updated for the version 4.7 public release to include enhanced emissions of sea-salt particles from the coastal surf zone and a chemically interactive coarse particle mode that enables dynamic transfer of HNO_3, H_2SO_4, HCl, and NH_3 between coarse particles and the gas phase. The updated version of CMAQ is applied to the Tampa Bay region, and predictions of size-composition distributions and gas-particle partitioning are evaluated against measurements from the BRACE campaign in May 2002. Results from the updated model are compared with results from CMAQv4.6 to demonstrate the model improvements and computational efficiency. Comparisons with observations are used to identify areas for future model development.

2 Modeling

2.1 Aerosol modeling

A brief description of CMAQ's aerosol module is given here; see Binkowski and Roselle (2003) for further details. CMAQ represents the atmospheric particle distribution as the superposition of three log-normal modes. The ISORROPIAv1.7 thermodynamic model (Nenes et al., 1998) is used to equilibrate inorganic components of the two fine modes with their gaseous counterparts. In CMAQv4.6 and prior model versions, the coarse particle mode is treated as dry and chemically inert with a fixed geometric standard deviation (GSD) of 2.2. These assumptions have been relaxed in the updates for CMAQv4.7 described in this paper. In the remainder of Section 2.1, the dynamically interactive coarse particle mode used in CMAQv4.7 is described along with changes to the treatment of particle-distribution GSDs. The parameterization of sea-salt emissions from the coastal surf zone used in CMAQv4.7 is described in Section 2.2. Additional scientific updates to CMAQ that were released in version 4.7 are described by Foley et al. (2009).

2.1.1 Dynamically interactive coarse particle mode

Wexler and Seinfeld (1990) demonstrated that time scales for gas-particle equilibration are long compared to those of other processes for certain atmospheric conditions. Allen et al. (1989) and Wexler and Seinfeld (1992) found evidence of departures from equilibrium, possibly due to mass-transfer limitations, in field studies of gas and particle systems. Meng and Seinfeld (1996) calculated that submicron particles in the atmosphere rapidly attain equilibrium with the gas phase, but that coarse particles generally exist in non-equilibrium transition states. Evidence from these and other studies suggests that models of coarse sea-salt chemistry must simulate gas-particle mass transfer rather than assuming instantaneous gas-particle equilibrium.

Simulating the dynamics of gas-particle mass transfer is challenging, because some components of the system equilibrate significantly faster than others and require small integration steps to be used for the entire system (i.e., the condensation-evaporation equations are stiff). Since component vapor pressures must be determined at each step using a computationally-intensive thermodynamic module, small time steps make the integration impractical for many air quality applications. A number of studies have proposed approximate techniques for expediting this integration: e.g., Sun and Wexler (1998a), Capaldo et al. (2000), Jacobson (2005), Zhang and Wexler (2006), and Zaveri et al. (2008). The "hybrid approach" of Capaldo et al. (2000) and Pilinis et al. (2000) is adopted in CMAQv4.7, since it has been used with success in a number of previous studies (e.g., Gaydos et al., 2003; Koo et al., 2003; Zhang et al., 2004; Sartelet et al., 2006, 2007; Athanasopoulou et al., 2008).

Two main sources of stiffness must be overcome when integrating the condensation-evaporation equations. First, fine particles equilibrate relatively quickly with the gas phase compared to coarse particles due in part to the higher surface area-to-volume ratios of fine particles. Second, the hydrogen ion concentration changes faster than concentrations of other components because the flux of hydrogen ion is determined by the sum of the fluxes of H_2SO_4, HNO_3, HCl, and NH_3, and the hydrogen ion concentration is relatively small (Sun and Wexler, 1998a; Zaveri et al., 2008). To minimize stiffness, two key assumptions are made in the hybrid approach of CMAQv4.7: (1) fine particle modes are in instantaneous equilibrium with the gas phase (Capaldo et al., 2000), and (2) condensation (evaporation) of HNO_3, HCl, and NH_3 to (from) the coarse particle mode is limited such that the flux of hydrogen ion is a maximum of 10% of the current hydrogen ion concentration per second (Pilinis et al., 2000).

The first assumption can introduce error into calculations when the fine modes are not in equilibrium with the gas phase. However, CMAQ's fine modes largely describe submicron particles with equilibration time scales comparable to those of typical gas/particle dynamics and often shorter than an operator step of 5-10 min (Meng and Seinfeld, 1996; Dassios and Pandis, 1999). The partitioning algorithm for the fine modes involves a bulk equilibrium calculation for the combined modes and a subsequent apportioning of mass to each mode using weighting factors based on the modal transport moments (Pandis et al., 1993; Binkowski and Shankar, 1995). Combining modes for the bulk equilibrium calculation produces error when the modes have different composition. While this source of error may be important for finely resolved sectional models, it is not significant in CMAQ, where the overwhelming proportion of fine mass resides in a single mode (i.e., the accumulation mode). Error may also be introduced into calculations by the decoupling of interactions between the gas phase and the fine and coarse modes over the operator time step. Capaldo et al. (2000) reported that error due to this decoupling became important for a 10-min operator step when a large spike of NH_3 was emitted during a challenging portion of their box-model simulation. However, the error was largely attributed to differences in particle phase state for different decoupling times. Since crystallization of inorganic salts is not modeled in CMAQ, CMAQ's aerosol calculations are much less sensitive to decoupling time than are calculations of the more detailed model of Capaldo et al. (2000).

Pilinis et al. (2000) performed sensitivity runs to evaluate the impact of the flux limit for the hydrogen ion (i.e., assumption (2) above). They reported that varying the limiter from 1% s^{-1} to 100% s^{-1} had little impact on results. To ensure the soundness of the approach, we confirmed that our predictions converge to the ISORROPIA equilibrium values after long integration times and agree with results based on a simplified version of the Jacobson (2005) method. Based on this evidence and the success of previous studies mentioned above, the artificial flux limitation of Pilinis et al. (2000) appears to be a reasonable method for maintaining numerical stability while performing integrations at long time step in air quality models. CMAQv4.7 uses a constant time step of 90 s for integrating the condensation-evaporation equations for coarse-mode particles.

2.1.2 Particle distribution geometric standard deviations

In CMAQv4.6, the GSD of the coarse particle mode is fixed at 2.2 and sulfate is the only component to influence GSDs of the fine modes during condensation and evaporation. In CMAQv4.7, the GSD of all three modes is variable; however, a constraint is imposed such that GSDs do not change during condensation and evaporation calculations. Except for the variable GSD of the coarse mode and the condensation-evaporation constraint, GSDs are calculated in CMAQv4.7 the same way as in previous CMAQ versions (Binkowski and Roselle, 2003). The constraint on GSDs during condensation and evaporation calculations is a temporary patch required to achieve stable GSD predictions, and its implications are discussed in Section 4.2.

2.1.3 Modeling chloride displacement from sea salt

In CMAQv4.7, HNO_3, HCl, and NH_3 condense and evaporate from the coarse particle mode and H_2SO_4 condenses. The primary advantage of the chemically-active coarse mode is that displacement of chloride by nitrate can be simulated in environments where sea-salt particles interact with pollutants from urban areas. Displacement of nitrate and chloride by sulfate is also simulated for coarse particles in CMAQv4.7; however, sulfate preferentially resides in the fine modes due to its negligible vapor pressure and the large surface area of the fine modes.

For solid NaCl particles exposed to HNO_3 at low relative humidity (RH), the replacement of chloride by nitrate is often expressed by the following heterogeneous reaction:

$$NaCl(s) + HNO_3(g) \rightarrow NaNO_3(s) + HCl(g) \qquad (R1)$$

(Beichert and Finlayson-Pitts, 1996). However, sea salt generally contains highly hygroscopic salts such as calcium and magnesium chloride in addition to sodium chloride. These salts have low deliquescence RHs (~33% for $MgCl_2.6H_2O$ and ~28% for $CaCl_2.6H_2O$ at 298 K, compared to ~75% for NaCl), and so the mutual deliquescence RH of the sea-salt mixture should be about 30% for typical coastal conditions (e.g., see Figs. 10-12 of Kelly and Wexler, 2006). Also, electrodynamic balance studies indicate that NaCl-$MgCl_2$ and $CaCl_2$ particles exist as supersaturated solutions at RHs well below their deliquescence RH under laboratory conditions (Cohen et al., 1987; Chan et al., 2000). Therefore, sea-salt particles are likely to contain an aqueous electrolyte solution at RH conditions typical of coastal environments, and the displacement of chloride by nitrate will often occur via solution thermodynamics rather than (R1).

Although CMAQ does not directly treat calcium or magnesium salts, inorganic particle components are assumed to exist in aqueous solution at all RHs using the "metastable" branch of the ISORROPIA model. The pathway for nitrate replacement of chloride in sea-salt particles in CMAQ is similar to that described by Jacobson (1997). As nitric acid condenses on a sea-salt particle to maintain equilibrium with the gas phase, the particle solution concentrates. The solution may concentrate further if the ambient RH subsequently decreases. For typical compositions, the activity coefficient of dissolved HCl increases dramatically compared to that of dissolved HNO_3 with increasing ionic strength (Jacobson, 1997; Dasgupta et al., 2007). Increases in activity cause the chemical potential of dissolved HCl to exceed that of gas-phase HCl, and some HCl evaporates to maintain equilibrium. Evaporation of HCl leads to lower ionic strength and enables nitrate to remain in solution. The overall change in particle composition for this process resembles that of (R1); however, chloride replacement in CMAQ is reversible and driven by solution thermodynamics rather than being a kinetically-limited forward reaction.

2.2 Parameterization of sea-salt emissions

Beginning with version 4.5, CMAQ has included online calculation of sea-salt emissions from the open ocean using the method of Gong (2003), who extended the parameterization of Monahan et al. (1986) to submicron sizes. This approach is based on the whitecap method, where the emission flux scales linearly with the fraction of ocean area covered by whitecaps. Over the open ocean, whitecap coverage is determined as a function of wind speed using the empirical relation of Monahan et al. (1986). The size distribution of emitted sea salt is adjusted to local RH before mixing it with the ambient particle modes (Zhang et al. 2005).

In CMAQ, primary sea-salt particles are speciated into three components (weight % by dry mass): Na^+ (38.56%), Cl^- (53.89%), and SO_4^{2-} (7.55%). This speciation represents non-sodium sea-salt cations (e.g., Mg^{2+}, Ca^{2+}, and K^+) by equivalent concentrations of sodium (on a mol basis) to achieve electroneutrality with the Cl^- and SO_4^{2-} anions. Moya et al. (2001) demonstrate that this approach is a good approximation when using thermodynamic aerosol models that do not include all crustal elements (e.g., see Fig. 2 of Moya et al, 2001). To recover the sodium fraction

of sea-salt cations for comparison with observations, the modeled sodium concentration (i.e., sodium plus non-sodium sea-salt cations) is multiplied by a factor of 0.78 during post-processing.

To account for enhanced sea-salt emission from the surf zone, Nolte et al. (2008) used the flux parameterization of de Leeuw et al. (2000). That treatment yielded relatively unbiased model results for total sodium when compared with observations at three BRACE sites. However, recent improvements to the spatial allocation of surf-zone grid cells resulted in several cells close to BRACE sampling sites being reclassified as surf-zone cells (see article supplement for details on surf-zone allocation). In preliminary simulations based on the de Leeuw et al. (2000) parameterization with the newly gridded surf zone, large over-predictions of sodium and chloride were found at the coastal Azalea Park site. Therefore a different approach was needed in this study. Surf-zone emissions are strongly dependent on local features such as wave height and bathymetry (de Leeuw et al., 2000; Lewis and Schwartz, 2004), but the de Leeuw et al. (2000) parameterization was based on measurements along the California coast and may not be suitable for the Florida coast. For instance, Petelski and Chomka (1996) observed significantly lower mass fluxes for the Baltic coast than were observed by de Leeuw et al. (2000) for California (see discussion in de Leeuw et al., 2000). However, de Leeuw et al. (2000) demonstrated compatibility between their surf-zone source function and several open-ocean source functions by assuming 100% whitecap coverage for the surf zone.

In CMAQv4.7, surf-zone emission fluxes are calculated using the open-ocean source function of Gong (2003) with a fixed whitecap coverage of 100% and a 50-m-wide surf zone. In Fig. 1, this flux is compared with the surf-zone source function of de Leeuw et al. (2000) and the Clarke et al. (2006) function based on 100% whitecap coverage. The Clarke et al. (2006) source function was developed for use in both open-ocean and coastal surf-zone environments and is based on observations of emissions from waves breaking on a Hawaiian shore. All three source functions yield similar order of magnitude for a 10-m wind speed of 0.01 m/s (Fig. 1, top); however, the de Leeuw et al. (2000) emission flux is much larger than the others for a 10-m wind speed of 9 m/s (Fig. 1, bottom). Note that the Gong (2003) and Clarke et al. (2006) curves do not depend on wind speed in Fig. 1, because the whitecap coverage is fixed. Considering the limitations of surf-zone emission estimates (e.g., Lewis and Schwartz, 2004, Section 4.3.5) and the similarity of the Gong (2003) flux with that derived from the surf measurements of Clarke et al. (2006), our

treatment of sea-salt emission from the coastal surf-zone in CMAQv4.7 is reasonable. However, we will revisit this topic in the future as new approaches become more established.

2.3 Model application: Tampa, FL, May 2002

The meteorological fields used to drive the air quality model were generated with the 5th generation Penn State/NCAR Mesoscale Model (MM5) v3.6 (Grell et al., 1994). CMAQ-ready meteorological files were generated from the MM5 simulations of Nolte et al. (2008) using the Meteorology-Chemistry Interface Processor version 3.3. The meteorological model was configured with 30 vertical layers (11 layers in the lowest 1000 m and a surface layer nominally 38 m deep), the Pleim-Xiu planetary boundary layer and land-surface models, the Grell cloud parameterization, the rapid radiative transfer model, and the Reisner II microphysics parameterization. To ensure that the simulated fields reflected actual meteorology, the model used analysis and observation nudging of temperature and moisture at the surface and aloft, and of winds aloft.

An overview of CMAQ equations and algorithms is given by Byun and Schere (2006). For our study, CMAQ was configured to use the SAPRC99 gas-phase chemical mechanism (Carter, 2000) and the Euler Backward Iterative solver. The modeling period (21 April – 3 June 2002) and nested domains match those of Nolte et al. (2008). Specifically, the outer domain uses a 32 km × 32 km horizontal grid and covers the continental U.S., with temporally invariant vertical concentration profiles at the boundaries (Byun and Ching, 1999). The inner domain uses a 8 km × 8 km horizontal grid that covers the Southeast U.S. The inner domain is shown in Fig. 2 with markers for three BRACE observational sites. Initial and boundary conditions for the inner domain were created from simulations on the outer domain. CMAQ-ready emission files containing information on area, point, mobile, and biogenic sources (i.e., all sources except sea salt) were taken from Nolte et al. (2008)—see that study for details on emission inventories and uncertainty estimates.

2.4 CMAQ model versions

Three versions of CMAQ are used in this study: CMAQv4.6, CMAQv4.6b, and CMAQv4.6c. CMAQv4.6 is a standard release version and is configured as described above. CMAQv4.6b is

identical to CMAQv4.6 except that v4.6b incorporates the surf-zone emission parameterization developed for v4.7 and described in Section 2.2. The impact of surf-zone emissions of sea salt on predictions is evaluated by comparing results of CMAQv4.6b with those of CMAQv4.6. CMAQv4.6c is identical to CMAQv4.6b except that v4.6c incorporates the dynamically interactive coarse particle mode and GSD treatments developed for v4.7 and described in Sections 2.1.1 and 2.1.2. The impact of the interactive coarse mode and GSD treatments are evaluated by comparing results of CMAQv4.6c with those of CMAQv4.6b. CMAQv4.7 is not used in this study because it contains numerous model updates in addition to those under consideration (Foley et al., 2009). CMAQv4.6b and CMAQv4.6c are used here to isolate the impacts of the new treatment of sea-salt emissions and the dynamically interactive coarse particle mode. These model versions are available from the authors upon request. Note that the coarse particle mode is dry, chemically inert, and has a fixed GSD of 2.2 in both CMAQv4.6 and CMAQv4.6b. Table 1 summarizes differences of the model versions used here.

3. Observations

CMAQ predictions are compared with observations made at three sampling sites in the Tampa, FL region (Fig. 2): Azalea Park (27.78ºN, 82.74ºW), Gandy Bridge (27.89ºN, 82.54ºW), and Sydney (27.97ºN, 82.23ºW). Details on the dataset are available in Nolte et al. (2008), Arnold et al. (2007), Dasgupta et al. (2007), and Evans et al. (2004). Briefly, size-resolved measurements of inorganic PM concentration were made with four micro-orifice cascade impactors, which operated for 23 h per sample (Evans et al., 2004). Impactors had 8-10 fractionated stages ranging from 0.056 to 18 μm in D_{aero}, and two impactors were collocated at the Sydney site. Samples were collected during 23-h periods on 15 days (14 at Sydney) during 2 May – 2 June 2002. The sampling dates are given on figures in the supplement. At the Sydney site, total (i.e., D_{aero} 50% cut ~12.5 μm) nitrate was measured with 15-min resolution using a soluble particle collector and an ion chromatograph (Dasgupta et al., 2007) and nitric acid was measured continuously by denuder difference (Arnold et al., 2007).

4 Results

4.1 Predicted and measured total PM concentrations

CMAQv4.6 and CMAQv4.6b predictions of 23-h average total concentration (summed over all modes) of sodium and chloride are compared with 23-h average total observed concentration (summed over all impactor stages) in Fig. 3 for observation days in the time period 2-15 May 2002. Grid-cell average predictions are compared with point measurements at the BRACE sites in this study. The results in Fig. 3 demonstrate the impact of the surf-zone emission parameterization developed for CMAQv4.7. When surf-zone emissions are neglected (i.e., CMAQv4.6), the normalized mean bias (NMB) is –85% for sodium and –76% for chloride over all sites. When surf-zone emissions are added to the model (i.e., CMAQv4.6b), the sodium and chloride concentrations increase by a factor of 2.8. Despite this improvement, model predictions still fall below the observed sodium and chloride concentrations (NMB = –58% and –34% for sodium and chloride, respectively). This result suggests that sea-salt emissions are significantly underestimated and/or the deposition of coarse-mode particles is too rapid in CMAQ.

In Fig. 4, CMAQv4.6b and CMAQv4.6c predictions of 23-h average total concentration of SO_4^{2-}, NH_4^+, NO_3^-, Na^+, and Cl^- are compared with 23-h average observed concentrations at three sites for the time period 2 May – 2 June 2002. Summary statistics for these comparisons are provided in Table 2. Differences in predictions for CMAQv4.6b and CMAQv4.6c are due to the different treatments of coarse-particle chemistry and modal GSDs described above. The largest difference in performance between the models is for nitrate concentration. Across all sampling sites and dates, nitrate is underestimated by about a factor of 10 in CMAQv4.6b (NMB = –92%) and only a factor of two in CMAQv4.6c (NMB = –56%). This substantial improvement is due to the treatment of coarse particles as chemically active in v4.6c but not v4.6b. The remaining under-prediction of nitrate by CMAQv4.6c is comparable to that of sodium (NMB = –56% and –40% for nitrate and sodium, respectively). Since sodium is the predominant cation in the coarse particles, further improvement in nitrate predictions may require improvements in sea-salt emissions and/or deposition treatment. Despite the shortcomings of the predictions, CMAQv4.6c estimates for total nitrate and sodium concentration are a clear improvement over those of CMAQv4.6b.

The NMB and normalized mean error (NME) for CMAQv4.6c over all sites is improved compared to CMAQv4.6b for all components except chloride (Table 2, All Sites). The better performance of CMAQv4.6c for sodium is perhaps surprising, because sodium is non-volatile and its emissions are based on the same parameterization in v4.6b and v4.6c. As explained in Section 4.2, the higher predictions of sodium concentration by CMAQv4.6c than by CMAQv4.6b are largely due to the different treatments of GSD for the coarse particle mode. The slightly higher (and better) predictions of total sulfate concentration by CMAQv4.6c are also attributable to the different coarse-mode GSD treatments, because coarse sea-salt particles contain a small amount of primary sulfate (7.6% by dry mass in CMAQ). Predictions of total ammonium concentration are essentially the same for CMAQv4.6b and CMAQv4.6c, and predictions of total chloride concentration are strongly biased low for both models at the Gandy Bridge and Sydney sites (Table 2). Due to the low bias in chloride predictions, replacement of chloride by nitrate in CMAQv4.6c results in slightly worse total chloride predictions for v4.6c than v4.6b at these sites. However, compared to standard CMAQv4.6, which does not account for the enhanced emission of sea salt from the surf zone, CMAQv4.6c predictions of chloride concentration are an improvement (e.g., see Table S1 in the supplement).

Comparing results across sites in Fig. 4, one notices that sodium predictions are increasingly biased low with distance from the Gulf of Mexico. Error in transport and deposition of sea-salt particles from the gulf could be responsible for this behavior. A related possibility is that relatively fine-scale coastal processes are not adequately captured with the 8-km horizontal resolution used in this study. Also, error in sea-salt emissions from the bay, which are calculated according to the open-ocean algorithm, could potentially lead to spatial differences in performance. For instance, bay emissions would impact the Gandy Bridge site most due to its bayside location (Fig. 2) and would influence the Sydney and Azalea Park sites differently for flows to and away from the gulf.

Overall, results in Fig. 4 and Table 2 indicate that the dynamically interactive coarse particle mode developed for CMAQv4.7 greatly improves predictions of total nitrate concentration and slightly improves predictions of total sulfate, ammonium, and sodium concentration near the coast. Results in Fig. 3 and Table S1 indicate that the surf-zone emission parameterization

developed for CMAQv4.7 improves predictions of total sodium and chloride concentration near the coast.

4.2 Predicted and measured particle size distributions

Size distributions of SO_4^{2-}, NH_4^+, NO_3^-, Na^+, and Cl^- predicted by CMAQv4.6b and CMAQv4.6c are compared with speciated impactor measurements averaged over all sampling days in Fig. 5. Modeled diameters were converted to D_{aero} for comparison with the impactor data. Since the four impactors did not have identical size cuts, observations were averaged to the size grid of a lower-resolution (8 fractionated stages) impactor for this figure. A figure similar to Fig. 5, but with CMAQ distributions mapped to the 8-stage size grid, is given in the supplement (Fig. S1). Comparisons of model predictions with observations at the original impactor resolutions for individual sampling days are also available in the supplementary material (Figs. S2-S15).

Both CMAQv4.6b and CMAQv4.6c correctly predict that ammonium and sulfate reside predominantly in fine particles (see top two panels of Fig. 5). CMAQv4.6b predicts higher distribution peaks for these species than does CMAQv4.6c. This difference is due in part to differences in the treatments of GSDs for the particle distributions. CMAQv4.6b allows fine mode GSDs to vary during sulfate condensation calculations, whereas CMAQv4.6c does not. Condensational growth narrows a size distribution, because the diameters of small particles increase relatively quickly compared to those of large particles due to the higher surface area-to-volume ratios of small particles. Therefore CMAQv4.6b predicts slightly narrower fine particle modes and higher size distribution peaks than does CMAQv4.6c: the average GSD of the accumulation mode is 2.02 for CMAQv4.6b and 2.05 for CMAQv4.6c over all sites and sampling days. Another potential reason for higher peaks in the ammonium and sulfate distributions of CMAQv4.6b is that small amounts of ammonia and sulfuric acid condense on coarse particles in CMAQv4.6c reducing their availability for condensation on fine particles. However, the mass of ammonium in the coarse mode is on average only 3% of that in the fine modes, and so uptake of ammonia by the coarse mode does not significantly impact the fine particle distribution. Similarly, the mass of sulfate in the coarse mode is small and due in part to primary emissions of sulfate in coarse sea-salt particles.

The largest difference in the size-distribution predictions of CMAQv4.6b and CMAQv4.6c is for nitrate. The chemically active coarse mode enables CMAQv4.6c to correctly predict that nitrate predominantly resides in coarse particles (Fig. 5). CMAQv4.6b does not allow the formation of coarse particle nitrate and cannot realistically simulate the nitrate size distribution at these three coastal observation sites. Despite the better performance of CMAQv4.6c for nitrate, under-prediction of sodium, the primary coarse particle cation, leads to under-prediction of coarse nitrate. At the Sydney site, the models under-predict sodium and nitrate in the coarse mode and over-predict nitrate in the accumulation mode (Fig. 5). The prediction of significant accumulation-mode nitrate at Sydney (but not the other sites) is primarily due to concentrations of ammonia in excess of those required to fully neutralize aqueous sulfuric acid at Sydney. The average predicted molar ratio of total ammonia (i.e., $NH_3 + NH_4^+$) to non-sea-salt SO_4^{2-} is greater than four at the Sydney site and only about two at Azalea Park and Gandy Bridge. Ammonia ratios greater than two exceed that of neutral $(NH_4)_2SO_4$ and facilitate nitric acid condensation by enabling significant neutralization of aqueous nitric acid. Over-prediction of accumulation-mode nitrate is more pronounced for CMAQv4.6b than CMAQv4.6c, because CMAQv4.6b does not have a pathway for coarse-mode nitrate formation.

Both models correctly predict that sodium and chloride reside predominantly in coarse particles (see bottom two panels of Fig. 5). However, CMAQv4.6c predicts higher concentrations of sodium than does CMAQv4.6b in better agreement with the measurements. Averaged over all sites and sampling days, the sodium concentration predicted by CMAQv4.6c is 32% greater than that predicted by CMAQv4.6b. Since emissions of sea salt are based on the same parameterization in CMAQv4.6b and CMAQv4.6c, differences in sodium predictions are attributable to differences in advective transport and deposition. The combined effect of these processes differs for the models largely because CMAQv4.6b uses a fixed GSD of 2.2 for the coarse particle mode, while CMAQv4.6c uses a variable coarse-mode GSD, which has an average value of 2.06 during the observation period. The lower coarse-mode GSD for CMAQv4.6c appears to result in lower dry deposition and in better predictions of coarse sodium concentration by v4.6c than v4.6b.

Both models over-predict the geometric mean diameter (GMD) of the accumulation mode (Figs. 5 and S1). Over-prediction of GMD also occurs for the coarse mode (see Figs. S2-S15 for

individual days); however, this behavior is not evident in Fig. 5, because the impactor measurements have been averaged to an 8-stage size distribution. Over-prediction of GMD could cause over-prediction of dry deposition and increasing low bias of concentration predictions with distance from a source. The peaks in the observed size distributions of sulfate and ammonium occur in the size bin with GMD of 0.40 μm. For CMAQ distributions that have been mapped to the impactor size grid (Fig. S1), the modeled peaks for sulfate and ammonium occur in the adjacent larger bin, which has a GMD of 0.75 μm. Although this difference could suggest an over-prediction of accumulation mode GMD of about 0.35 μm or 88% by CMAQ, the exact over-prediction cannot be quantified due to the limited impactor resolution and the different representations of the particle size distribution by CMAQ and the cascade impactor. Similarly, GSD of the accumulation mode appears to be over-predicted by CMAQ based on visual inspection of Figs. 5 and S1, but the exact over-prediction cannot be reliably quantified.

Since fine and coarse particles have different sources, the over-prediction of GMD is not easily attributable to an incorrect emission size distribution. Modal GMD is diagnosed from the zeroth, second and third moments of the particle size distribution in CMAQ, and so the cause of the diameter over-prediction is not obvious. Zhang et al. (2006) reported similar over-prediction of volume mean diameter by CMAQ for a site in Atlanta in summer, and Elleman and Covert (2009) reported that CMAQ size distributions are shifted to larger sizes compared with observations at Langley, Bristish Columbia in August. Therefore the problem of diameter over-prediction is not confined to conditions of the BRACE campaign. Note that $PM_{2.5}$ predictions would increase slightly if over-predictions of GMD were corrected, because a larger fraction of the accumulation mode would fall below 2.5 μm (Jiang et al., 2006). Also note that predictions of D_{aero} for coarse particle modes by CMAQv4.6b and CMAQv4.6c are similar even though the coarse mode does not contain water in v4.6b. In the calculation of D_{aero}, the relatively low density of water compared to that of dry sea-salt components compensates for the larger Stokes diameters predicted by CMAQv4.6c.

4.3 Predictions and measurements of nitrate partitioning

Predictions of the mass fraction of nitrate in the particle phase [i.e., $NO_3^- / (HNO_3 + NO_3^-)$] are compared with highly time-resolved measurements made at the Sydney site in Fig. 6. The average value of the particle fraction of nitrate over the observation period is 0.51 for the measurements, 0.35 for CMAQv4.6c, and 0.13 for CMAQv4.6b. Therefore the chemically-active coarse particle mode greatly improves predictions of nitrate partitioning by CMAQ. Despite this improvement, CMAQv4.6c generally under-predicts the particle fraction of nitrate. Also, although the timing of many peaks in the observed time series is correctly predicted, the diurnal amplitude of the measurements is not adequately captured by the model. However, CMAQv4.6c is a clear improvement over CMAQv4.6b, which incorrectly predicts that the particle fraction of nitrate is negligible for many time periods. CMAQv4.6c also provides better predictions of absolute concentrations of HNO_3 and HCl than CMAQv4.6b (e.g., see Figs. S16 and S17).

The under-prediction of the fraction of nitrate in the particle phase by CMAQv4.6c could be due to the under-prediction of sodium ion discussed above. To investigate this possibility, the average molar ratios of the inorganic ions to the sodium ion are examined for the two highest fractionated stages (1.8−3.2 and 3.2−18 μm; Fig. 7). CMAQ predictions were mapped to these stages by integrating the distributions in Fig. 5 over the impactor size ranges. The measured ammonium-to-sodium ratios are negligible for these stages and suggest that sodium is the dominant cation for $D_{aero} > 3.2$ μm. In contrast to the observations, both CMAQv4.6b and CMAQv4.6c predict amounts of ammonium and sulfate comparable to that of sodium in the lower of the two size bins (Fig. 7, bottom two rows). This behavior is attributable to the over-prediction of GMD, and possibly GSD, by CMAQ (Figs. 5 and S1). The error in CMAQv4.6c predictions of the molar ratios of nitrate and chloride to sodium for the lower stage (Fig. 7, top two rows) may reflect a limitation of using a single mode to represent all coarse particles.

Since the models correctly predict that the ammonium-to-sodium ratios are negligibly small for the highest stage, the influence of sodium on nitrate partitioning predictions can be evaluated by focusing on this stage. If under-prediction of nitrate is primarily a consequence of under-prediction of sodium, the nitrate-to-sodium ratios should be in reasonable agreement with the observations. For the Gandy Bridge and Sydney sites, CMAQv4.6c predictions of the nitrate-to-sodium ratio agree well with observations despite the large under-prediction of absolute nitrate

concentration. The nitrate-to-sodium molar ratio is under-predicted by CMAQv4.6c by only 0.5% at Gandy Bridge and by only 7.5% at Sydney, whereas absolute nitrate concentration is under-predicted by 53% at Gandy Bridge and 57% at Sydney. The molar ratios of the other inorganic ions are also in reasonable agreement with measurements at these sites. Therefore the under-prediction of nitrate and particle fraction of nitrate by CMAQv4.6c is largely attributable to the under-prediction of sodium ion. This finding suggests that the dynamically interactive coarse particle mode is functioning properly, but that emissions, transport, and deposition of sodium are not adequately captured by the model for the Tampa domain. In contrast to the good predictions for the Gandy Bridge and Sydney sites, the nitrate-to-sodium molar ratio is under-predicted by 49% by CMAQv4.6c at Azalea Park. The Azalea Park site is located in a grid cell with surf-zone emissions of sea salt, and so the error in the modeled nitrate-to-sodium ratio at this site may reflect the poor representation of the mixing of marine and continental air masses in the grid cell. However, the good predictions of the nitrate-to-sodium ratio at the inland (Sydney) and non-surf-zone bay site (Gandy Bridge) indicate that the sea-salt chemical-processing calculations are reliable.

4.4 Model timing

Computational efficiency is a key aspect of the model developments described here. Models that are significantly slower than CMAQv4.6 are not suitable for conducting the numerous long-term simulations required for developing State Implementation Plans for the annual $PM_{2.5}$ standard. The run time of CMAQv4.6c is only about 8% longer than that of CMAQv4.6. This increase is modest considering the significantly better predictions of CMAQv4.6c at the coastal BRACE sites. The primary cause of the longer run time for CMAQv4.6c is the additional calls to the ISORROPIA thermodynamic module used in simulating dynamic mass transfer of coarse-particle components in CMAQv4.6c.

5 Closing remarks

This study focuses on evaluating parameterizations of sea-salt emissions from the coastal surf zone and the dynamic transfer of HNO_3, H_2SO_4, HCl, and NH_3 between coarse particles and the

gas phase in CMAQ. The methods described above improve predictions of inorganic particle components and nitrate partitioning at sites near Tampa Bay, FL and are included in the public release of CMAQ version 4.7. While the updates to CMAQ clearly improve predictions for conditions of the BRACE campaign, several areas for future model development were identified.

First, particle size distributions from CMAQ do not adequately capture the narrow distribution peaks of the observations. The opposite problem (i.e., modeled distributions too narrow) was reported by Nolte et al. (2008) for a simulation of the same domain with the CMAQ-UCD model. The causes of this difference should be determined in a future study. Second, particle-mode GMDs are over-predicted by CMAQ. Considering that Zhang et al. (2006) and Elleman and Covert (2009) also report over-prediction of diameter by CMAQ and that this discrepancy may influence $PM_{2.5}$ predictions, the source of the error should be investigated in future work.

Another area for future model development is on improving the simulation of sea-salt emissions from the coastal surf zone. The surf-zone emission parameterization developed for CMAQv4.7 improves predictions of sodium and chloride concentration in the Tampa area. Yet predictions of sodium are increasingly biased low with distance from the Gulf of Mexico. This behavior was not observed in the Nolte et al. (2008) study and could be due to inadequate sea-salt emissions in addition to the over-predictions of GMD and GSD, which could yield too rapid particle deposition rates. The Clarke et al. (2006) parameterization (Fig. 1) produces higher sea-salt emissions than the modified Gong (2003) function used in CMAQv4.7 and could improve predictions for the Tampa domain. However, emissions of sea salt from the surf zone are dependent on local features, and the ideal parameterization for Tampa may not be suitable for other locations where CMAQ is applied. Possibly, a parameterization could be developed that adapts to local features, or multiple parameterizations could be incorporated into CMAQ and applied separately in different parts of the domain.

In addition to the emission parameterization, error in sodium and chloride predictions can be attributed to using 8 km × 8 km horizontal grid cells for simulating relatively fine-scale coastal processes. Athanasopoulou et al. (2008) recently used 2 km × 2 km horizontal grid cells in a nested portion of their domain to capture fine-scale processes near the coast. Predictions were not evaluated quantitatively in that study, because measurements are not available during the simulation period. Using higher grid resolution and tuning sea-salt emission from the surf zone

could result in better predictions of the BRACE observations. However, the goal of our development is a model that can be applied generally by CMAQ users, who are often constrained to coarse grid resolutions and do not focus on the Tampa area.

While the model updates are evaluated here for conditions of Tampa, a separate study (Foley et al., 2009) suggests that the updates improve model performance in several coastal environments. In that study, CMAQv4.7 simulations with and without the new model features are performed for the eastern U.S. with 12-km horizontal resolution, and predictions are compared with observations from nine coastal CASTNET (Clarke et al., 1997) and four coastal SEARCH (Hansen et al., 2003) sites. For the CASTNET sites, the updated sea-salt emissions and coarse particle processes decrease the mean absolute error (MAE) for nitric acid predictions by 36% in January and by 33% in August 2006, while MAE for total particle nitrate decreases by 10% in January and by 1% in August 2006. For the SEARCH sites, the model updates decrease MAE for coarse particle nitrate by 45% in January and by 52% in August 2006, while MAE for fine particle nitrate decreases by 0.5% in January and by 11% in August 2006. These simulations are thoroughly discussed by Foley et al. (2009). The comparisons with coastal CASTNET and SEARCH observations build confidence that the modeling approaches described here improve CMAQ predictions across a range of coastal conditions. However, accurate prediction of fine-scale coastal processes probably requires using higher grid resolution and a surf-zone emission parameterization tailored to local conditions.

Acknowledgments

We kindly thank the following individuals for their assistance in conducting this study: W. Benjey, R. Dennis, A. Eyth, E. Kinnee, R. Mathur, S. Pandis, T. Pierce, G. Pouliot, S. Roselle, K. Sartelet, K. Schere, and M. Wilson.

Disclaimer

The United States Environmental Protection Agency through its Office of Research and Development funded and managed the research described here. It has been subjected to the Agency's administrative review and approved for publication.

References

Allen, A. G., Harrison, R. M., and Erisman, J. W.: Field-measurements of the dissociation of ammonium-nitrate and ammonium-chloride aerosols, Atmos. Environ., 23(7), 1591-1599, 1989.

Arnold, J. R., Hartsell, B. E., Luke, W. T., Ullah, S. M. R., Dasgupta, P. K., Huey, L. G., and Tate, P.: Field test of four methods for gas-phase ambient nitric acid, Atmos. Environ., 41(20), 4210-4226, 2007.

Asgharian, B., Hoffman, W., and Bergmann, R.: Particle deposition in a multiple-path model of the human lung, Aerosol Sci. and Technol., 34, 332-339, 2001.

Athanasopoulou, E., Tombrou, M., Pandis, S. N., and Russell, A. G.: The role of sea-salt emissions and heterogeneous chemistry in the air quality of polluted coastal areas, Atmos. Chem. Phys., 8, 5755-5769, 2008.

Atkeson, T., Greening, H., and Poor, N.: Bay Region Atmospheric Chemistry Experiment (BRACE), Atmos. Environ., 41(20), 4163-4164, 2007.

Beichert, P., and Finlayson-Pitts, B. J.: Knudsen cell studies of the uptake of gaseous HNO3 and other oxides of nitrogen on solid NaCl: The role of surface-adsorbed water, J. Phys. Chem., 100(37), 15218-15228, 1996.

Bessagnet, B., Hodzic, A., Vautard, R., Beekmann, M., Cheinet, S., Honoré, C., Liousse, C., and Rouil, L.: Aerosol modeling with CHIMERE—preliminary evaluation at the continental scale, Atmos. Environ., 38(18), 2803-2817, 2004.

Binkowski, F. S., and Roselle, S. J.: Models-3 community multiscale air quality (CMAQ) model aerosol component - 1. Model description, J.Geophys. Res. 108(D6), 4183-4201, 2003.

Bricker, S., Longstaff, B., Dennison, W., Jones, A., Boicourt, K., Wicks, C., and Woerner, J.: Effects of Nutrient Enrichment In the Nation's Estuaries: A Decade of Change, NOAA Coastal Ocean Program Decision Analysis Series No. 26, National Centers for Coastal Ocean Science, Silver Spring, MD, 2007.

Binkowski, F., and Shankar, U.: The Regional Particulate Matter Model 1. Model description and preliminary results, J. Geophys. Res., 100(D12), 26191-26209, 1995.

Brunekreef, B., and Forsberg, B.: Epidemiological evidence of effects of coarse airborne particles on health, European Respiratory J., 26(2), 309-318, 2005.

Byun, D., and Ching, J. K. S.: Science algorithms of the EPA Models-3 Community Multiscale Air Quality (CMAQ) modeling system, Tech. Rep. EPA-600/R-99/030, U.S. Government Printing Office, U.S. Environmental Protection Agency, Washington, D.C, 1999.

Byun, D., and Schere, K. L.: Review of the governing equations, computational algorithms, and other components of the Models-3 Community Mulitiscale Air Quality (CMAQ) modeling system, Appl. Mech. Rev., 59, 51-77, 2006.

Capaldo, K. P., Pilinis, C., and Pandis, S. N.: A computationally efficient hybrid approach for dynamic gas/aerosol transfer in air quality models, Atmos. Environ., 34(21), 3617-3627, 2000.

Carter, W. P. L.: Implementation of the SAPRC-99 chemical mechanism into the Models-3 framework, Tech. Rep., U.S. Environmental Protection Agency. URL: http:/www.cert.ucr.edu/~carter/absts.htm#s99mod3, 2000.

Chan, C. K., Ha, Z. Y., and Choi, M. Y.: Study of water activities of aerosols of mixtures of sodium and magnesium salts, Atmos. Environ., 34(28), 4795-4803, 2000..

Clarke, J. F., Edgerton, E. S., and Martin, B. E.: Dry deposition calculations for the clean air status and trends network, Atmos. Environ., 31(21), 3667-3678, 1997.

Clarke, A. D., Owens, S. R., and Zhou, J. C.: An ultrafine sea-salt flux from breaking waves: Implications for cloud condensation nuclei in the remote marine atmosphere, J. Geophys. Res., 111, D06202, doi:10.1029/2005JD006565, 2006.

Cohen, M. D., Flagan, R. C., and Seinfeld, J. H.: Studies of concentrated electrolyte-solutions using the electrodynamic balance.1. Water activities for single-electrolyte solutions, J. Phys. Chem., 91(17), 4563-4574, 1987.

Dasgupta, P. K., Campbell, S. W., Al-Horr, R. S., Ullah, S. M. R., Li, J. Z., Amalfitano, C., and Poor, N. D.: Conversion of sea salt aerosol to $NaNO_3$ and the production of HCl: analysis of temporal behavior of aerosol chloride/nitrate and gaseous HCl/HNO_3, Atmos. Environ., 41(20), 4242-4257, 2007.

Dassios, K. G., and Pandis, S. N.: The mass accommodation coefficient of ammonium nitrate aerosol, Atmos. Environ., 33(18), 2993-3003, 1999.

de Leeuw, G., Neele, F. P., Hill, M., Smith, M. H., and Vignati, E.: Production of sea spray aerosol in the surf zone, J. Geophys. Res., 105(D24), 29397-29409, 2000.

Evans, M. S. C., Campbell, S. W., Bhethanabotla, V., and Poor, N. D.: Effect of sea salt and calcium carbonate interactions with nitric acid on the direct dry deposition of nitrogen to Tampa Bay, Florida, Atmos. Environ., 38(29), 4847-4858, 2004.

Elleman, R. A., and Covert, D. S.: Aerosol size distribution modeling with the Community Multiscale Air Quality modeling system (CMAQ) in the Pacific Northwest: 1. Model comparison to observations, J. Geophys. Res., 114, D11206, doi:10.1029/2008 JD010791, 2009.

Foley, K. M., Roselle, S. J., Appel, K. W., Bhave, P. V., Pleim, J. E., Otte, T. L., Mathur, R., Sarwar, G., Young, J. O., Gilliam, R. C., Nolte, C. G., Kelly, J. T., Gilliland, A. B., and Bash, J. O.: Incremental testing of the community multiscale air quality (CMAQ) modeling system version 4.7, Geosci. Model Dev. Discuss., 2, 1245-1297, 2009.

Foltescu, V.L., Pryor, S. C., and Bennet, C.: Sea salt generation, dispersion and removal on the regional scale, Atmos. Environ., 39(11), 2123-2133, 2005.

Gard, E. E., Kleeman, M. J., Gross, D. S., Hughes, L. S., Allen, J. O., Morrical, B. D., Fergenson, D. P., Dienes, T., Galli, M. E., Johnson, R. J., Cass, G. R., and Prather, K. A.: Direct observation of heterogeneous chemistry in the atmosphere, Science, 279, 1184-1187, 1998.

Gaydos, T. M., Koo, B., Pandis, S. N., and Chock, D. P.: Development and application of an efficient moving sectional approach for the solution of the atmospheric aerosol condensation/evaporation equations, Atmos. Environ., 37(23), 3303-3316, 2003.

Gong, S. L.: A parameterization of sea-salt aerosol source function for sub- and super-micron particles, Global Biogeochem. Cycles, 17(4), 1097, doi: 10.1029/2003GB002079, 2003.

Grell, G., Dudhia, J., and Stauffer, D.: A description of the fifth-generation Penn State/NCAR mesoscale model (MM5), Tech. Rep. NCAR/TN-398+STR, National Center for Atmospheric Research, Boulder, CO, 1994.

Grell, G. A., Peckham, S. E., Schmitz, R., McKeen, S. A., Frost, G., Skamarock, W. C., and Eder, B.: Fully coupled “online” chemistry within the WRF model, Atmos. Environ., 39(37), 6957-6975, 2005.

Hansen, D. A., Edgerton, E .S., Hartsell, B. E., Jansen, J. J., Kandasamy, N., Hidy, G. M., and Blanchard, C. L.: The southeastern aerosol research and characterization study: Part 1-Overview, J. Air Waste Manag. Assoc., 53(12):1460-71, 2003.

Hopkins, R. J., Desyaterik, Y., Tivanski, A. V., Zaveri, R. A., Berkowitz, C. M., Tyliszczak, T., Gilles, M. K., and Laskin, A.: Chemical speciation of sulfur in marine cloud droplets and particles: Analysis of individual particles from the marine boundary layer over the California current, J. Geophys. Res., 113, D04209, doi:10.1029/2007JD008954, 2008.

Hsu, S.-C., Liu, S. C., Kao, S.-J., Jeng, W.-L., Huang, Y.-T., Tseng, C.-M., Tsai, F., Tu, J.-Y., and Yang, Y.: Water-soluble species in the marine aerosol from the northern South China Sea: High chloride depletion related to air pollution, J. Geophys. Res., 112, D19304, doi:10.1029/2007JD008844, 2007.

Jacobson, M. Z.: Development and application of a new air pollution modeling system.3. Aerosol-phase simulations, Atmos. Environ., 31(4), 587-608, 1997.

Jacobson, M. Z.: A solution to the problem of nonequilibrium acid/base gas-particle transfer at long time step, Aerosol Sci. Technol., 39(2), 92-103, 2005.

Jiang, W., Smyth, S., Giroux, É, Roth, H., and Yin, D.: Differences between CMAQ fine mode particle and PM2.5 concentrations and their impact on model performance evaluation in the lower Fraser valley, Atmos. Environ., 40(26), 4973-4985, 2006

Keene W. C., Stutz, J., Pszenny, A. A. P., Maben, J. R., Fischer, E. V., Smith, A. M., von Glasow, R., Pechtl, S., Sive, B. C., and Varner, R. K.: Inorganic chlorine and bromine in coastal New England air during summer, J. Geophys. Res., 112, D10S12, doi:10.1029/2006JD007689, 2007.

Kelly, J. T., and Wexler, A. S.: Water uptake by aerosol: Water activity in supersaturated potassium solutions and deliquescence as a function of temperature, Atmos. Environ., 40(24), 4450-4468, 2006.

Kleeman, M. J., and Cass, G. R.: A 3D Eulerian source-oriented model for an externally mixed aerosol, Environ. Sci. Technol., 35, 4834-4848, 2001.

Koo, B., Gaydos, T. M., and Pandis, S. N.: Evaluation of the equilibrium, dynamic, and hybrid aerosol modeling approaches, Aerosol Sci. Technol., 37(1), 53-64, 2003.

Lee, T., Yu, X. Y., Ayres, B., Kreidenweis, S. M., Malm, W. C., and Collett, J. L.: Observations of fine and coarse particle nitrate at several rural locations in the United States, Atmos. Environ., 42(11), 2720-2732, 2008.

Lewis, E. R., and Schwartz, S. E.: Sea-Salt Aerosol Production: Mechanisms, Methods, Measurements, and Models--A Critical Review. American Geophysical Union, Washington, D. C, 2004.

Lurmann, F. W., Wexler, A. S., Pandis, S. N., Musarra, S., Kumar, N., Seinfeld, J. H.: Modelling urban and regional aerosols.2. Application to California's South Coast Air Basin, Atmos. Environ., 31(17), 2695-2715, 1997.

McInnes, L. M., Covert, D. S., Quinn, P. K., and Germani, M. S.: Measurements of chloride depletion and sulfur enrichment in individual sea-salt particles collected from the remote marine boundary-layer, J. Geophys., 99(D4), 8257-8268, 1994.

Meng, Z. Y., Dabdub, D., Seinfeld, J. H.: Size-resolved and chemically resolved model of atmospheric aerosol dynamics, J. Geophys. Res., 103(D3), 3419-3435, 1998.

Meng, Z. Y., and Seinfeld, J. H.: Time scales to achieve atmospheric gas-aerosol equilibrium for volatile species, Atmos. Environ., 30(16), 2889-2900, 1996.

Monahan, E. C., Spiel, D. E., and Davidson, K. L.: A model of marine aerosol generation via whitecaps and wave disruption. In: Monahan, E.C., MacNiocaill, G., (Eds.), Oceanic Whitecaps. D. Reidel Publishing Company. Norwell, Mass.: pp. 167-174, 1986.

Moya, M., Ansari, A. S., and Pandis, S. N.: Partitioning of nitrate and ammonium between the gas and particulate phases during the 1997 IMADA-AVER study in Mexico City, Atmos. Environ., 35, 1791-1804, 2001.

Nenes, A., Pandis, S. N., and Pilinis, C.: ISORROPIA: A new thermodynamic equilibrium model for multiphase multicomponent inorganic aerosols, Aquatic Geochem., 4(1), 123-152, 1998.

Nicholls, R. J., and Small, C.: Improved estimates of coastal population and exposure to hazards released, EOS Transactions, July, 83(28), 301 & 305, 2002.

Nolte, C. G., Bhave, P. V., Arnold, J. R., Dennis, R. L., Zhang, K. M., and Wexler, A. S.: Modeling urban and regional aerosols - Application of the CMAQ-UCD Aerosol Model to Tampa, a coastal urban site, Atmos. Environ., 42(13), 3179-3191, 2008.

Osthoff, H. D., Roberts, J. M., Ravishankara, A. R., Williams, E. J., Lerner, B. M., Sommariva, R., Bates, T. S., Coffman, D., Quinn, P. K., Dibb, J. E., Stark, H., Burkholder, J. B., Talukdar, R. K., Meagher, J., Fehsenfeld, F. C., and Brown, S. S.: High levels of nitryl chloride in the polluted subtropical marine boundary layer, Nature Geosci., 1(5), 324-328, 2008.

Pandis, S. N., Wexler, A. S., and Seinfeld, J. H.: Secondary organic aerosol formation and transport.2. predicting the ambient secondary organic aerosol-size distribution, Atmos. Environ., 27(15), 2403-2416, 1993.

Park, S. K., Marmur, A., Kim, S. B., Tian, D., Hu, Y. T., McMurry, P. H., and Russell, A. G.: Evaluation of fine particle number concentrations in CMAQ, Aerosol Sci. Technol., 40(11), 985-996, 2006.

Petelski, T., and Chomka, M.: Marine aerosol fluxes in the coastal zone--BAEX experimental data, Oceanologia, 38, 469-484, 1996.

Pierce, J. R., and Adams, P. J.: Global evaluation of CCN formation by direct emission of sea salt and growth of ultrafine sea salt, J. Geophys. Res., 111, D06203, doi:10.1029/2005JD006186, 2006.

Pilinis, C., Capaldo, K. P., Nenes, A., and Pandis, S. N.: MADM - A new multicomponent aerosol dynamics model, Aerosol Sci. and Technol., 32(5), 482-502, 2000.

Pleim, J., Wong, D., Mathur, R., Young, J., Otte, T., Gilliam, R., Binkowski, F., and Xiu, A.: Development of the coupled 2-way WRF-CMAQ system, 7th Annual CMAS Conference. October 6-8, Chapel Hill, NC, http://www.cmascenter.org, 2008.

Pryor, S. C., Barthelmie, R. J., Schoof, J. T., Binkowski, F. S., Delle Monache, L., and Stull, R.: Modeling the impact of sea-spray on particle concentrations in a coastal city, Sci. Tot. Environ., 391, 132-142, 2008.

Pryor, S. C., and Sorensen, L. L.: Nitric acid-sea salt reactions: Implications for nitrogen deposition to water surfaces, J. Appl. Meteorol., 39(5), 725-731, 2000.

Sandstrom, T., Nowak, D., and van Bree, L.: Health effects of coarse particles in ambient air: messages for research and decision-making, European Respiratory J., 26(2), 187-188, 2005.

Sartelet, K. N., Hayami, H., Albriet, B., and Sportisse, B.: Development and preliminary validation of a modal aerosol model for tropospheric chemistry: MAM, Aerosol Sci. Technol., 40(2), 118-127, 2006.

Sartelet, K. N., Hayami, H., and Sportisse, B.: Dominant aerosol processes during high-pollution episodes over Greater Tokyo, J. Geophys. Res., 112, D14214, doi:10.1029/2006JD007885, 2007.

Sarwar, G., and Bhave, P. V.,: Modeling the effect of chlorine emissions on ozone levels over the eastern United States, J. Appl. Meteorol. Climatol., 46(7), 1009-1019, 2007.

Seinfeld, J. H., and Pandis, S. N.: Atmospheric Chemistry and Physics: From Air Pollution to Climate Change. John Wiley & Sons, Inc., New York, 1998.

Simon, H., Kimura, Y., McGaughey, G., Allen, D. T., Brown, S. S., Osthoff, H. D., Roberts, J. M., Byun, D., and Lee, D.: Modeling the impact of ClNO2 on ozone formation in the Houston area, J. Geophys. Res., 114, D00F03, doi:10.1029/2008JD010732, 2009.

Smyth, S. C., Jiang, W. M., Roth, H., Moran, M. D., Makar, P. A., Yang, F. Q., Bouchet, V. S., and Landry, H.: A comparative performance evaluation of the AURAMS and CMAQ air-quality modelling systems, Atmos. Environ., 43(5), 1059-1070, 2009.

Spyridaki, A., Lazaridis, M., Eleftheriadis, K., Smolik, J., Mihalopoulos, N., and Aleksandropoulou, V.: Modelling and evaluation of size-resolved aerosol characteristics in the eastern Mediterranean during the SUB-AERO project, Atmos. Environ., 40, 6261-6275, 2006.

Sullivan, R. C., and Prather, K. A.: Investigations of the diurnal cycle and mixing state of oxalic acid in individual particles in Asian aerosol outflow, Environ. Sci. Technol., 41(23), 8062-8069, 2007.

Sun, Q., and Wexler, A. S.: Modeling urban and regional aerosols - Condensation and evaporation near acid neutrality, Atmos. Environ., 32(20), 3527-3531, 1998a.

Sun, Q., and Wexler, A. S.: Modeling urban and regional aerosols near acid neutrality - Application to the 24-25 June SCAQS episode, Atmos. Environ., 32(20), 3533-3545, 1998b.

Tang, I., Tridico, A., and Fung, K.: Thermodynamic and optical properties of sea salt aerosols, J. Geophys. Res., 102(D19), 23269-23275, 1997.

Volckens, J., Dailey, L., Walters, G., and Devlin R. B.: Direct particle-to-cell deposition of coarse ambient particulate matter increases the production of inflammatory mediators from cultured human airway epithelial cells, Environ. Sci. Technol., 43(12), 4595-4599, 2009.

Wexler, A. S., and Seinfeld, J. H.: The distribution of ammonium-salts among a size and composition dispersed aerosol, Atmos. Environ., 24(5), 1231-1246, 1990.

Wexler, A. S., and Seinfeld, J. H.: Analysis of aerosol ammonium-nitrate - departures from equilibrium during SCAQS, Atmos. Environ., 26(4), 579-591, 1992.

Zaveri, R. A., Easter, R. C., Fast, J. D., and Peters, L. K.: Model for Simulating Aerosol Interactions and Chemistry (MOSAIC). J. Geophys. Res., 113, D13204, doi:10.1029/2007JD008782, 2008.

Zhang, K. M., Knipping, E. M., Wexler, A. S., Bhave, P. V., and Tonnesen, G. S.: Size distribution of sea-salt emissions as a function of relative humidity, Atmos. Environ., 39(18), 3373-3379, 2005.

Zhang, K. M., and Wexler, A. S.: An asynchronous time-stepping (ATS) integrator for atmospheric applications: Aerosol dynamics, Atmos. Environ., 40(24), 4574-4588, 2006.

Zhang, K. M., and Wexler, A. S.: Modeling urban and regional aerosols - Development of the UCD Aerosol Module and implementation in CMAQ model, Atmos. Environ., 42(13), 3166-3178, 2008.

Zhang, Y., Liu, P., Pun, B., and Seigneur, C.: A comprehensive performance evaluation of MM5-CMAQ for the summer 1999 southern oxidants study episode- Part III: diagnostic and mechanistic evaluations, Atmos. Environ., 40(26), 4856-4873, 2006.

Zhang, Y., Pun, B., Vijayaraghavan, K., Wu, S. Y., Seigneur, C., Pandis, S. N., Jacobson, M. Z., Nenes, A., and Seinfeld, J. H.: Development and application of the model of aerosol dynamics,

reaction, ionization, and dissolution (MADRID), J. Geophys. Res., 109, D01202, doi:10.1029/2003JD003501, 2004.

Table 1.Differences in CMAQ model versions used in this study

Model[a]	Sea-Salt Emissions[b]	Coarse Particle Mode[c]	Fine-Mode GSD[d]	Coarse-Mode GSD[d]
CMAQv4.6	Open-ocean only	Dry, chemically inert	Variable, influenced by condensation of H_2SO_4	2.2
CMAQv4.6b	Open-ocean and coastal surf-zone	Dry, chemically inert	Variable, influenced by condensation of H_2SO_4	2.2
CMAQv4.6c	Open-ocean and coastal surf-zone	Wet, dynamic mass transfer of HNO_3, H_2SO_4, HCl, NH_3 between gas and particle phases	Variable, doesn't change during condensation or evaporation	Variable, doesn't change during condensation or evaporation

[a]CMAQv4.6 is a standard release version; CMAQv4.6b and CMAQv4.6c are non-standard versions created for this study to evaluate the updated sea-salt emission and coarse-particle chemistry parameterizations developed for CMAQv4.7.
[b]Open-ocean parameterization is that of Gong (2003); the coastal surf-zone parameterization uses the source function of Gong (2003) with 100% whitecap coverage and a 50-m-wide surf zone (Section 2.2).
[c]Dynamic mass transfer is calculated using the hybrid method of Capaldo et al. (2000) (Section 2.1.1)
[d]Particle distribution geometric standard deviations are discussed in Section 2.1.2.

Table 2. Mean observed (summed over all impactor stages) and model-predicted (summed over all modes) inorganic particle concentrations (μg m^{-3}) at three sites near Tampa, FL.

Species	Obs.[a]	$Mod_{v4.6b}$[b]	$Mod_{v4.6c}$	$R_{v4.6b}$[c]	$R_{v4.6c}$	$NMB_{v4.6b}$[d]	$NMB_{v4.6c}$	$NME_{v4.6b}$[e]	$NME_{v4.6c}$	$RMSE_{v4.6b}$[f]	$RMSE_{v4.6c}$
Azalea Park											
sulfate	4.03	3.71	3.82	0.45	0.45	-7.9	-5.3	40	39	2.1	2.1
ammonium	1.23	0.93	0.94	0.51	0.51	-24	-24	33	33	0.6	0.6
nitrate	1.96	0.09	0.81	-0.07	0.04	-96	-59	96	69	2.0	1.5
sodium	1.62	1.09	1.40	-0.06	-0.01	-33	-13	49	49	0.9	1.0
chloride	1.93	1.89	1.98	-0.04	0.09	-1.8	2.5	49	57	1.2	1.3
Gandy Bridge											
sulfate	4.08	4.21	4.28	0.44	0.43	3.2	5.1	43	42	2.3	2.3
ammonium	1.30	1.10	1.11	0.52	0.53	-15	-14	28	28	0.5	0.5
nitrate	1.74	0.06	0.82	-0.14	0.11	-96	-53	96	60	1.8	1.2
sodium	1.46	0.54	0.73	0.52	0.47	-63	-50	63	50	1.1	0.9
chloride	1.72	0.93	0.80	0.57	0.65	-46	-53	49	54	1.1	1.1
Sydney											
sulfate	3.13	2.59	2.66	0.47	0.46	-17	-15	30	30	1.2	1.2
ammonium	1.04	0.94	0.95	0.33	0.34	-8.8	-8.0	41	41	0.5	0.5
nitrate	1.51	0.30	0.65	-0.08	0.40	-80	-57	81	60	1.3	1.0
sodium	1.14	0.29	0.40	0.77	0.77	-75	-65	75	65	1.0	0.9
chloride	1.31	0.49	0.46	0.77	0.86	-63	-65	63	65	1.0	1.1
All Sites											
sulfate	3.76	3.52	3.61	0.49	0.48	-6.3	-4.1	39	38	1.9	1.9
ammonium	1.19	0.99	1.00	0.47	0.48	-17	-16	34	33	0.5	0.5
nitrate	1.74	0.15	0.77	-0.17	0.16	-92	-56	92	63	1.7	1.2
sodium	1.41	0.65	0.86	0.35	0.34	-54	-40	60	54	1.0	0.9
chloride	1.66	1.12	1.09	0.34	0.38	-33	-34	52	58	1.1	1.2

[a]Observed mean concentration (μg m^{-3})

[b]Modeled mean concentration (μg m^{-3}) for CMAQv4.6b

[c]Pearson correlation coefficient for CMAQv4.6b predictions

[d]Normalized mean bias (%) for CMAQv4.6b predictions; $NMB = \frac{\sum C_{\mathrm{mod}} - C_{obs}}{\sum C_{obs}} \times 100\%$, where C is concentration

[e]Normalized mean error (%) for CMAQv4.6b predictions; $NME = \frac{\sum |C_{\mathrm{mod}} - C_{obs}|}{\sum C_{obs}} \times 100\%$

[f]Root mean square error (μg m^{-3}) for CMAQv4.6b predictions; $RMSE = \sqrt{1/n \sum (C_{\mathrm{mod}} - C_{obs})^2}$, where n is the number of samples

Figure legends

Figure 1. Comparison of sea-salt emission size distributions at 80% RH with 10-m wind speed (U) of (a) 0.01 m/s and (b) 9 m/s. Clarke et al. (2006) and Gong (2003) source functions are based on 100% whitecap coverage; the magnitude of the de Leeuw et al. (2000) source function is wind-speed dependent.

Figure 2. Inner modeling domain (8 km × 8km) centered on Tampa, FL. Markers indicate land-based observational sites.

Fig. 3. Modeled total sodium and chloride particle concentrations vs. 23-h impactor observations at three Tampa-area sites for 5 sampling days (6 at Azalea Park) during 2-15 May 2002. 'v4.6' indicates CMAQv4.6; 'v4.6b' indicates CMAQv4.6b; see Table 1 for version description. For reference, the dashed line represents 1:1 ratio.

Figure 4. Modeled total inorganic particle concentrations vs. 23-h impactor observations at three Tampa-area sites for 15 sampling days (14 at Sydney) during 2 May – 2 June 2002. 'v4.6b' indicates CMAQv4.6b; 'v4.6c' indicates CMAQv4.6c; see Table 1 for version description. For reference, the dashed line represents 1:1 ratio. See Table 2 for summary statistics.

Figure 5. Observed and predicted size distributions of inorganic particle components at three Tampa-area sites averaged over 15 sampling days (14 at Sydney) during 2 May – 2 June 2002. Vertical dashed line indicates D_{aero} of 2.5 μm.

Figure 6. Time series of observed and modeled fraction of total nitrate in the particle phase [i.e., $NO_3^- / (HNO_3 + NO_3^-)$] at the Sydney, FL site from 1 May – 2 June 2002. Tick marks represent 0000 local standard time on each day.

Figure 7. Observed and modeled molar ratios of average inorganic ion concentration to average sodium ion concentration at three Tampa-area sites for 15 sampling days (14 at Sydney) during 2 May – 2 June 2002. Horizontal dashed lines indicate average Cl^- / Na^+ and SO_4^{2-} / Na^+ ratios in seawater.

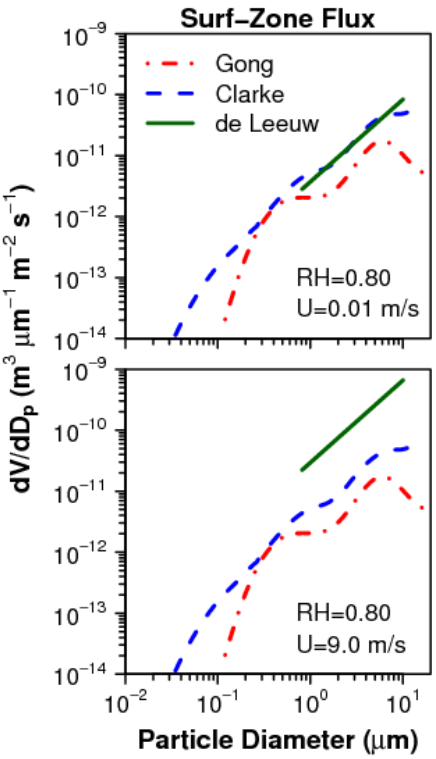
Surf–Zone Flux
Gong
Clarke
de Leeuw
RH=0.80
U=0.01 m/s
RH=0.80
U=9.0 m/s
dV/dDp (m3 µm-1 m-2 s-1)
Particle Diameter (µm)

Figure 1.

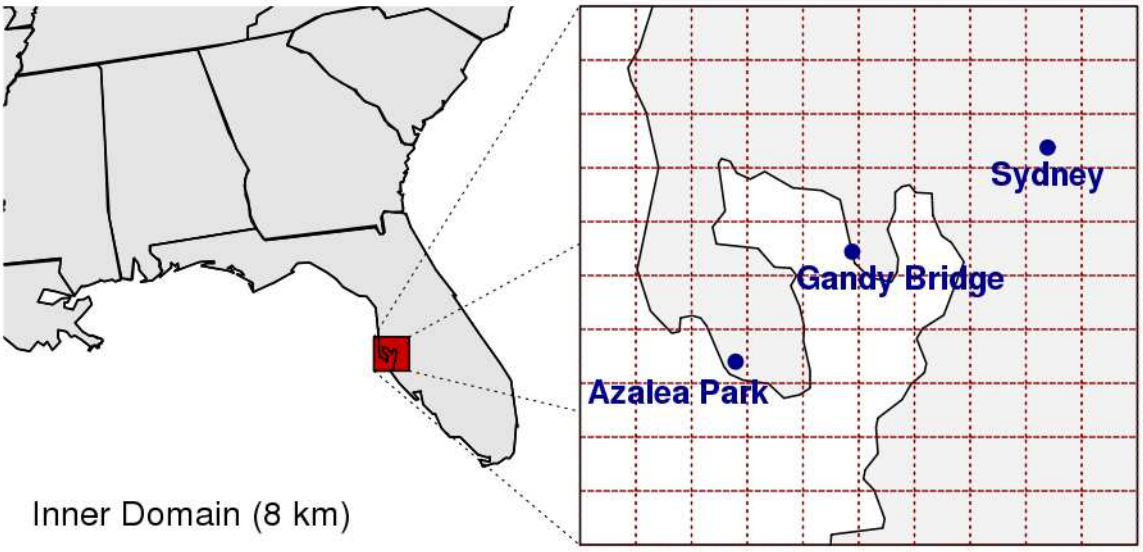

Figure 2.

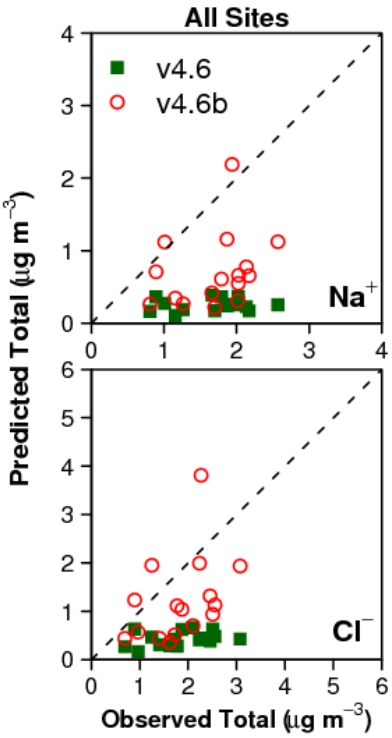
All Sites
v4.6
v4.6b
Na+
Cl−
Predicted Total (μg m−3)
Observed Total (μg m−3)

Fig. 3.

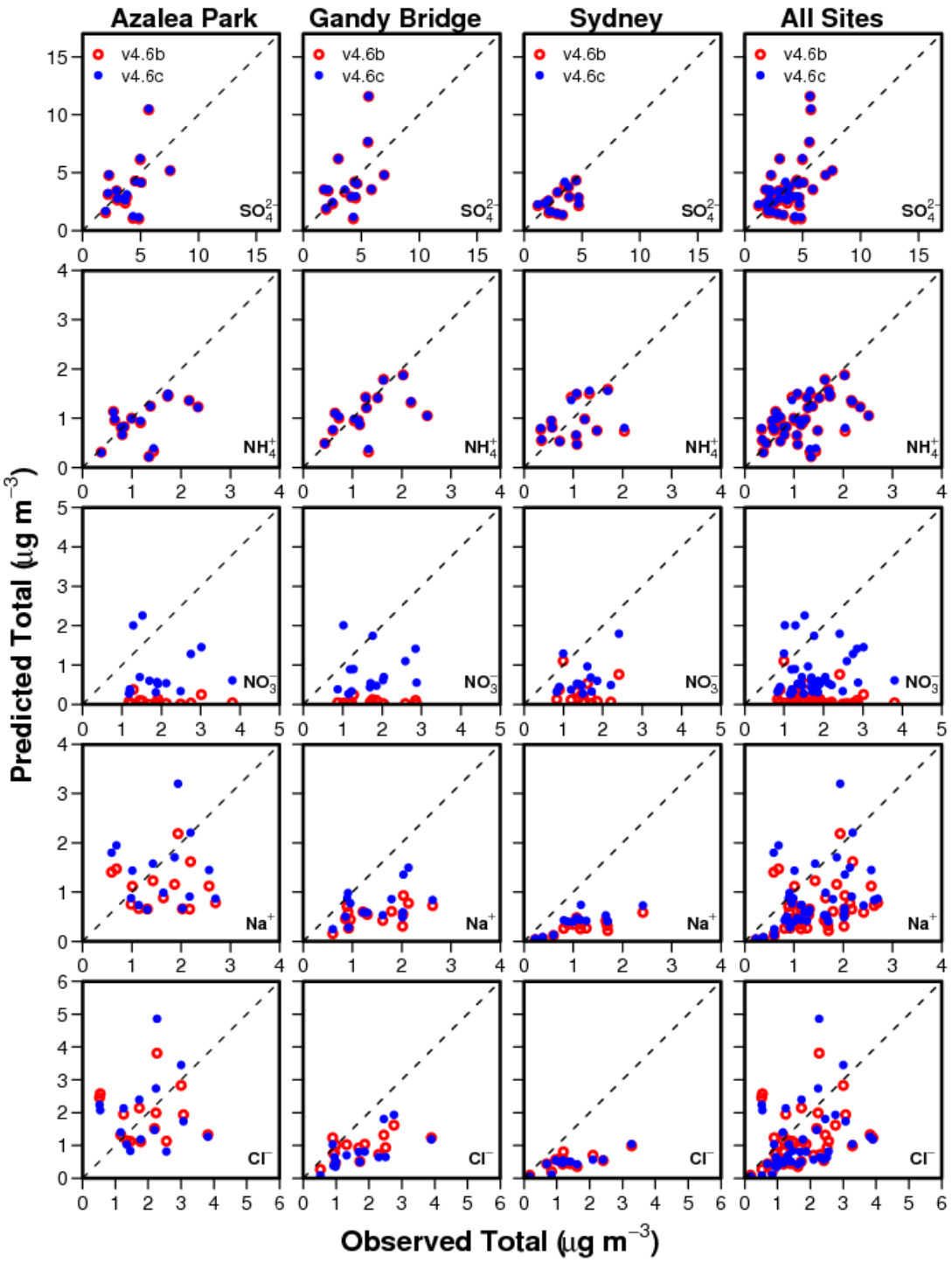
Azalea Park
Gandy Bridge
Sydney
All Sites
v4.6b
v4.6c
SO_4^{2-}
NH_4^+
NO_3^-
Na^+
Cl^-
Predicted Total (μg m^{-3})
Observed Total (μg m^{-3})

Figure 4.

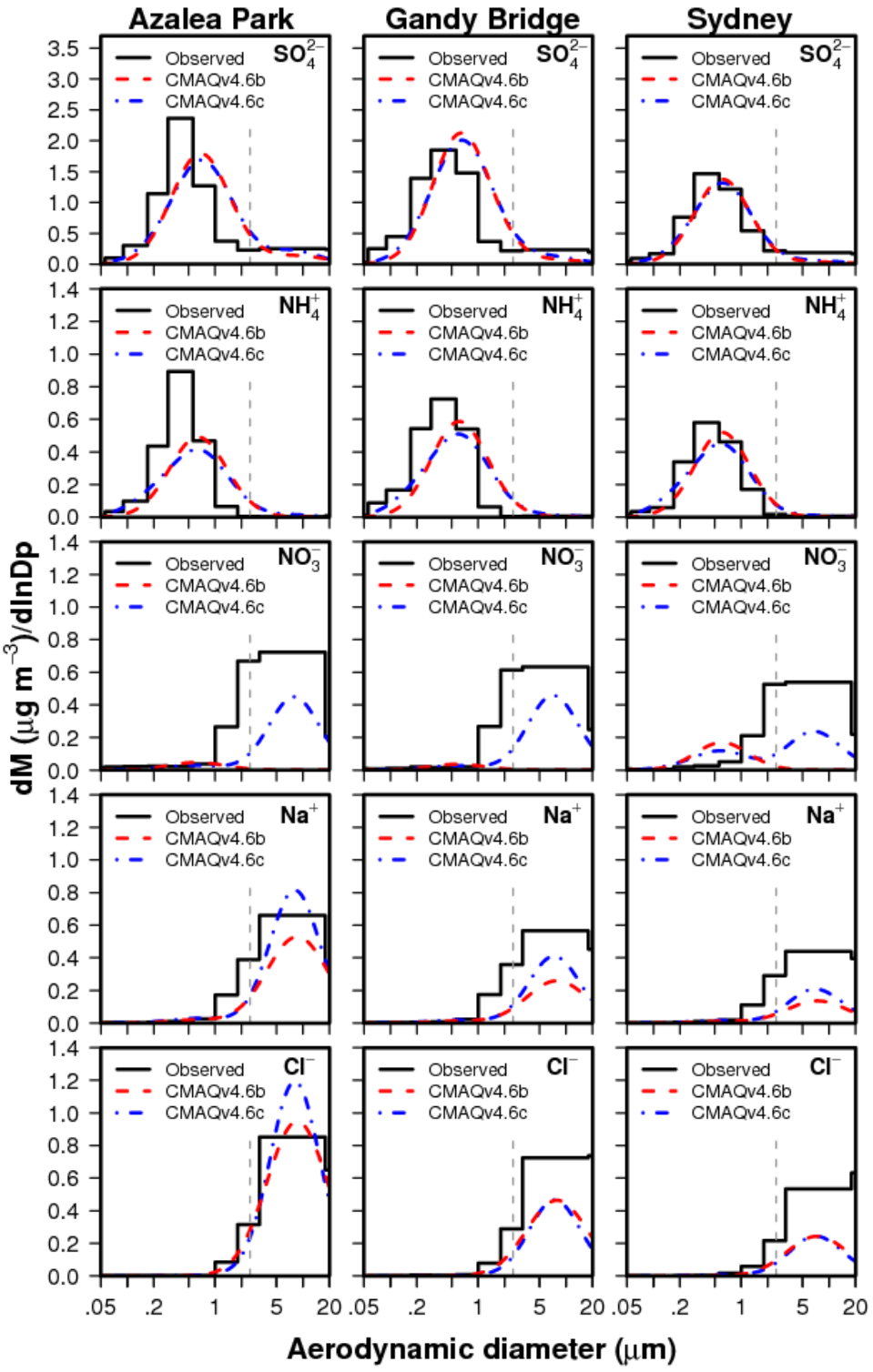
Azalea Park
Gandy Bridge
Sydney
Observed
CMAQv4.6b
CMAQv4.6c
SO_4^{2-}
NH_4^+
NO_3^-
Na^+
Cl^-
dM (μg m^{-3})/dlnDp
Aerodynamic diameter (μm)
.05
.2
1
5
20

Figure 5.

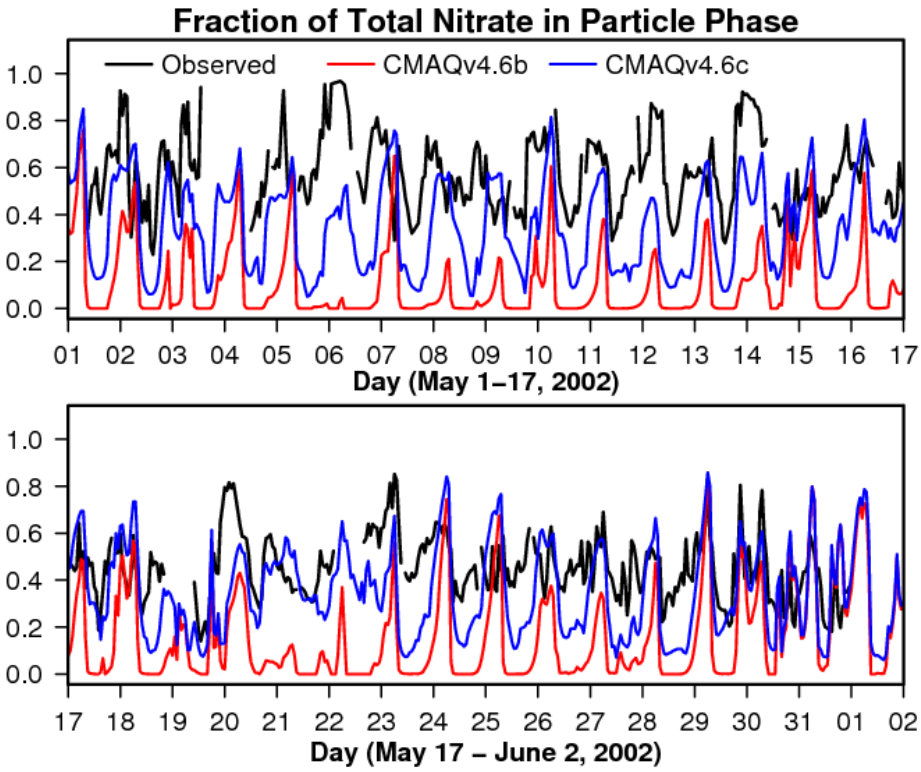
Fraction of Total Nitrate in Particle Phase
Observed
CMAQv4.6b
CMAQv4.6c
1.0
0.8
0.6
0.4
0.2
0.0
01 02 03 04 05 06 07 08 09 10 11 12 13 14 15 16 17
Day (May 1–17, 2002)
1.0
0.8
0.6
0.4
0.2
0.0
17 18 19 20 21 22 23 24 25 26 27 28 29 30 31 01 02
Day (May 17 – June 2, 2002)

Figure 6.

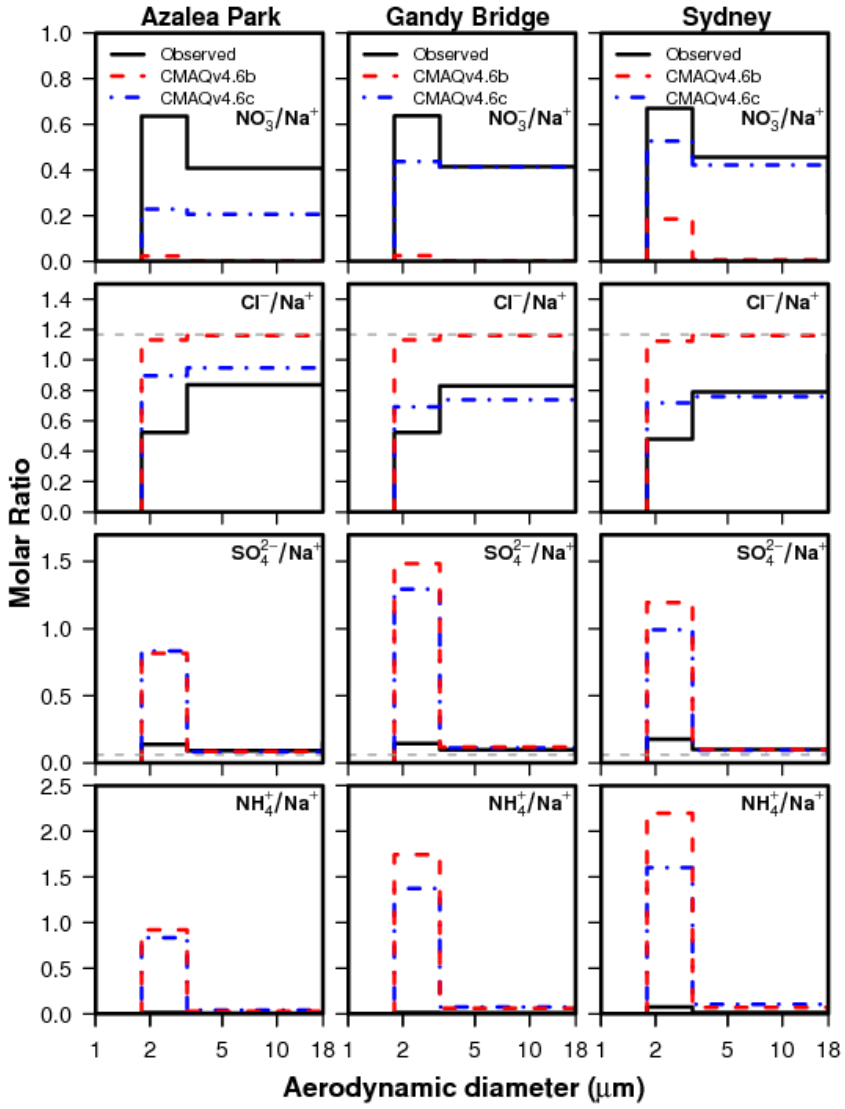
Azalea Park
Gandy Bridge
Sydney
Observed
CMAQv4.6b
CMAQv4.6c
NO_3^-/Na^+
Cl^-/Na^+
SO_4^{2-}/Na^+
NH_4^+/Na^+
Molar Ratio
Aerodynamic diameter (μm)

Figure 7.

Supplement to the research article:

Simulating emission and chemical evolution of coarse sea-salt particles in the Community Multiscale Air Quality (CMAQ) model

J. T. Kelly[1,*], P. V. Bhave[1], C. G. Nolte[1], U. Shankar[2], and K. M. Foley[1]

[1]*Atmospheric Modeling and Analysis Division, National Exposure Research Laboratory, Office of Research and Development, U.S. Environmental Protection Agency, RTP, NC*

[2]*Institute for the Environment, University of North Carolina, Chapel Hill, NC*

[*]*now at: Planning and Technical Support Division, Air Resources Board, California Environmental Protection Agency, Sacramento, CA*

Correspondence to J. T. Kelly (jkelly@arb.ca.gov)

Table S1. Mean observed (summed over all impactor stages) and model-predicted (summed over all modes) inorganic particle concentrations (μg m^{-3}) at three sites near Tampa, FL. Note that this table is for CMAQv4.6, CMAQv4.6b, and CMAQv4.6c during 2−15 May 2002, while Table 2 is for CMAQv4.6b and CMAQv4.6c during 2 May−2June 2002.

Species	Obs[a]	$Mod_{v4.6}$[b]	$Mod_{v4.6b}$	$Mod_{v4.6c}$	$R_{v4.6}$[c]	$R_{v4.6b}$	$R_{v4.6c}$	$NMB_{v4.6}$[d]	$NMB_{v4.6b}$	$NMB_{v4.6c}$
Azalea Park										
sulfate	4.46	3.34	3.42	3.53	0.21	0.19	0.18	-25.1	-23.3	-20.7
ammonium	1.28	0.94	0.9	0.9	0.24	0.25	0.24	-26.5	-29.5	-29.4
nitrate	2.6	0.07	0.08	0.82	-0.03	0.08	0.23	-97.3	-97	-68.5
sodium	1.93	0.25	1.15	1.56	-0.33	-0.1	-0.09	-87.2	-40.4	-19.1
chloride	2.19	0.42	1.99	2.24	0.19	0.06	-0.04	-80.9	-9.2	2.4
Gandy Bridge										
sulfate	4.55	4.23	4.23	4.31	-0.07	-0.09	-0.13	-7.1	-6.9	-5.2
ammonium	1.44	1.12	1.12	1.12	-0.05	-0.04	-0.09	-22.1	-22.4	-22.1
nitrate	2.31	0.05	0.05	0.92	-0.08	0.03	0.23	-98	-98	-60.3
sodium	1.77	0.32	0.59	0.86	-0.54	-0.31	0.07	-82.2	-66.7	-51.3
chloride	1.89	0.54	1.01	0.96	-0.32	-0.01	0.22	-71.3	-46.6	-49.2
Sydney										
sulfate	3.66	2.99	3.01	3.09	0.53	0.52	0.48	-18.3	-17.8	-15.6
ammonium	1.15	1.04	1.04	1.04	0.22	0.24	0.28	-9.5	-9.2	-9.5
nitrate	1.96	0.29	0.29	0.84	0.35	0.35	0.57	-85.4	-85.1	-57.3
sodium	1.32	0.2	0.3	0.51	0.56	0.19	-0.12	-84.6	-77	-61.6
chloride	1.36	0.34	0.5	0.5	0.81	0.41	0.38	-74.9	-62.9	-63.2
All Sites										
sulfate	4.23	3.51	3.54	3.64	0.22	0.22	0.2	-17.2	-16.3	-14.1
ammonium	1.29	1.03	1.01	1.01	0.17	0.18	0.18	-20.2	-21.4	-21.3
nitrate	2.31	0.13	0.14	0.86	-0.11	-0.08	0.24	-94.3	-94.1	-63
sodium	1.69	0.25	0.71	1.01	0.14	0.28	0.27	-84.9	-57.9	-40
chloride	1.84	0.43	1.22	1.3	0.33	0.4	0.34	-76.4	-33.6	-29.3

[a]Observed mean concentration (μg m^{-3})

[b]Modeled mean concentration (μg m^{-3}) for CMAQv4.6

[c]Pearson correlation coefficient for CMAQv4.6 predictions

[d]Normalized mean bias (%) for CMAQv4.6 predictions; $NMB = \frac{\sum C_{\mathrm{mod}} - C_{obs}}{\sum C_{obs}} \times 100\%$, where C is concentration

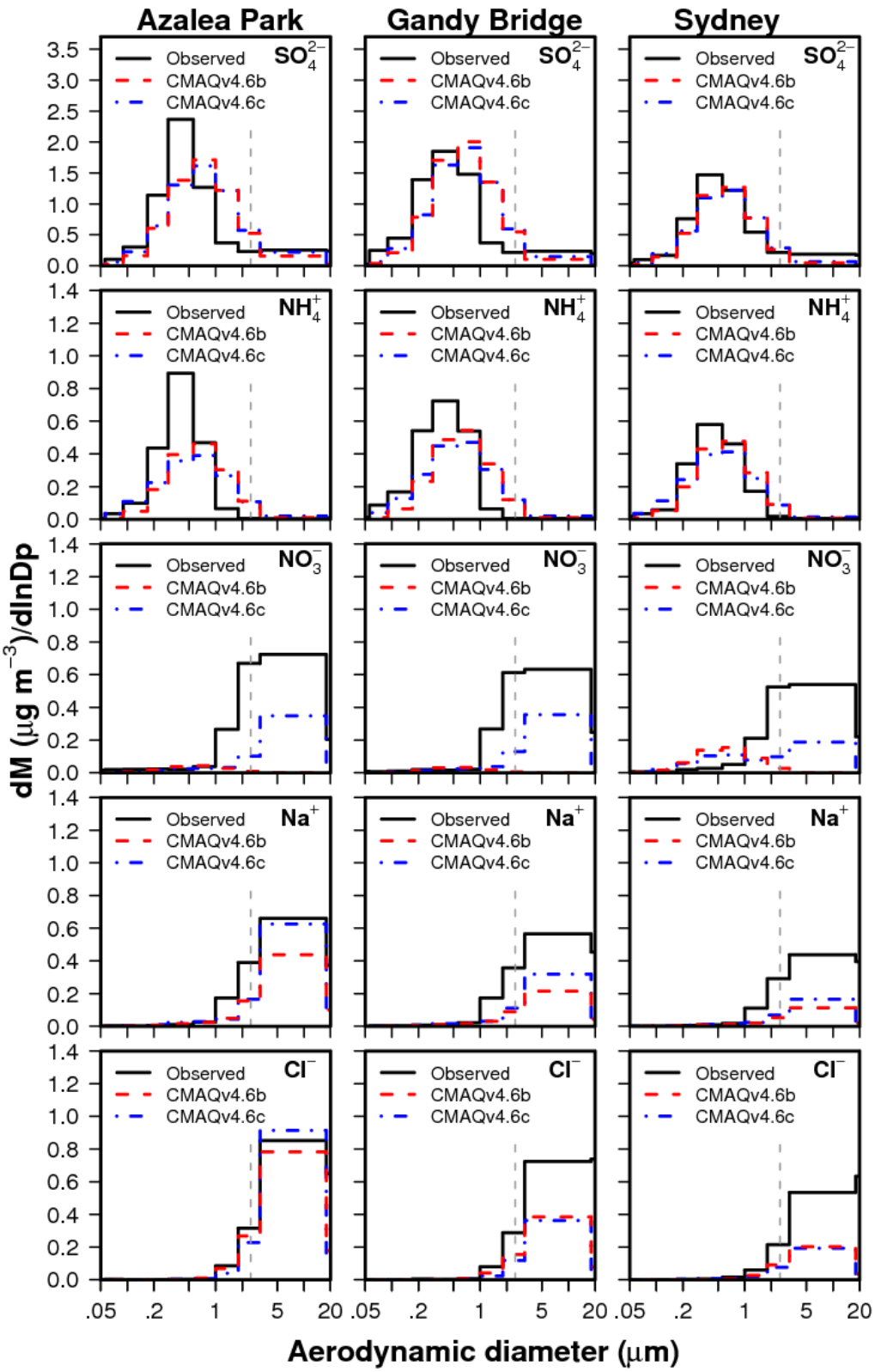

Fig. S1. Same as Fig.5 but with modeled distributions mapped to bins by integrating over relevant diameter ranges.

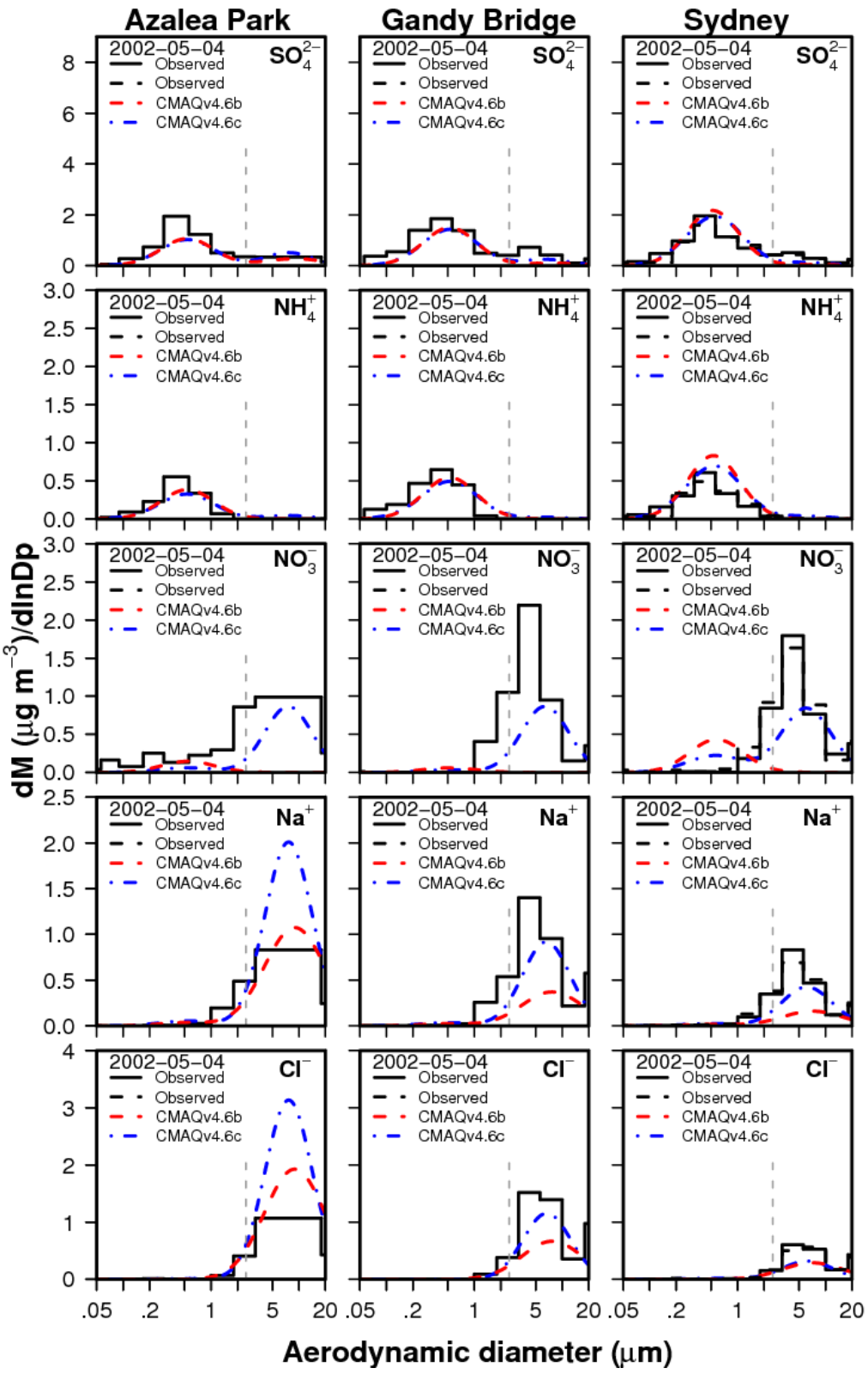

Fig. S2. Observed and predicted size distributions of inorganic particle components at three Tampa-area sites averaged over a 23-h period on 4 May 2002.

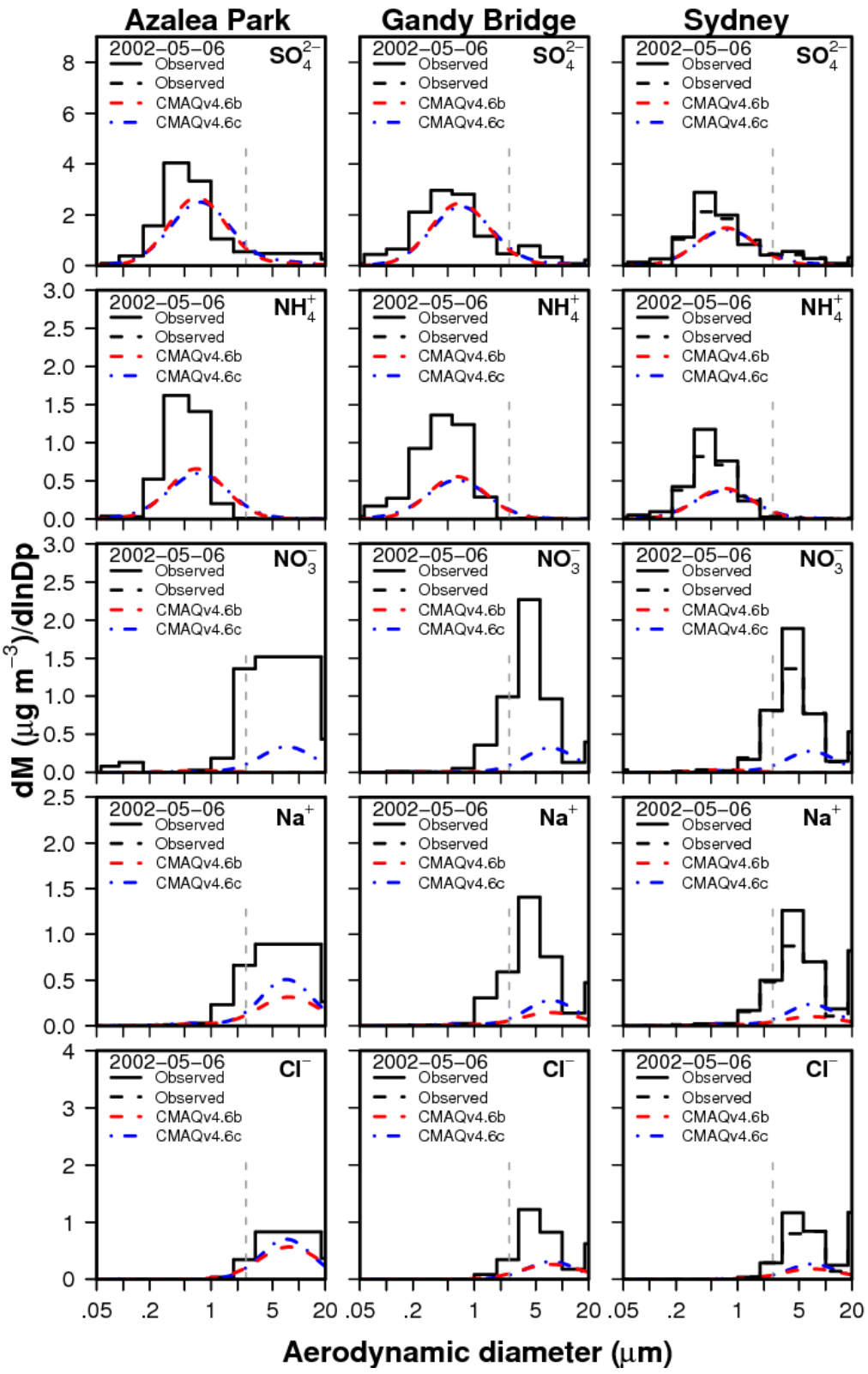

Fig. S3. Observed and predicted size distributions of inorganic particle components at three Tampa-area sites averaged over a 23-h period on 6 May 2002.

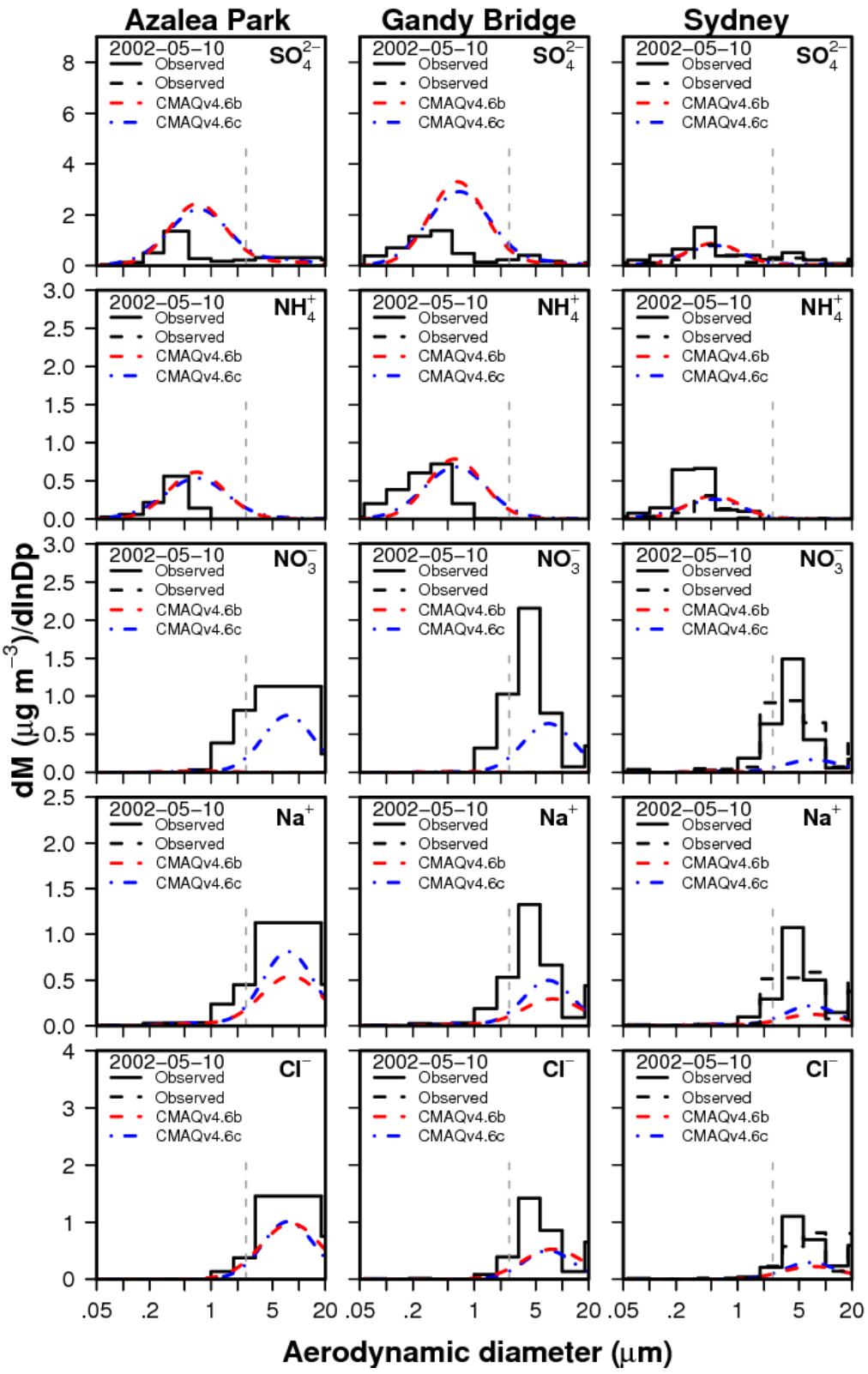

Fig. S4. Observed and predicted size distributions of inorganic particle components at three Tampa-area sites averaged over a 23-h period on 10 May 2002.

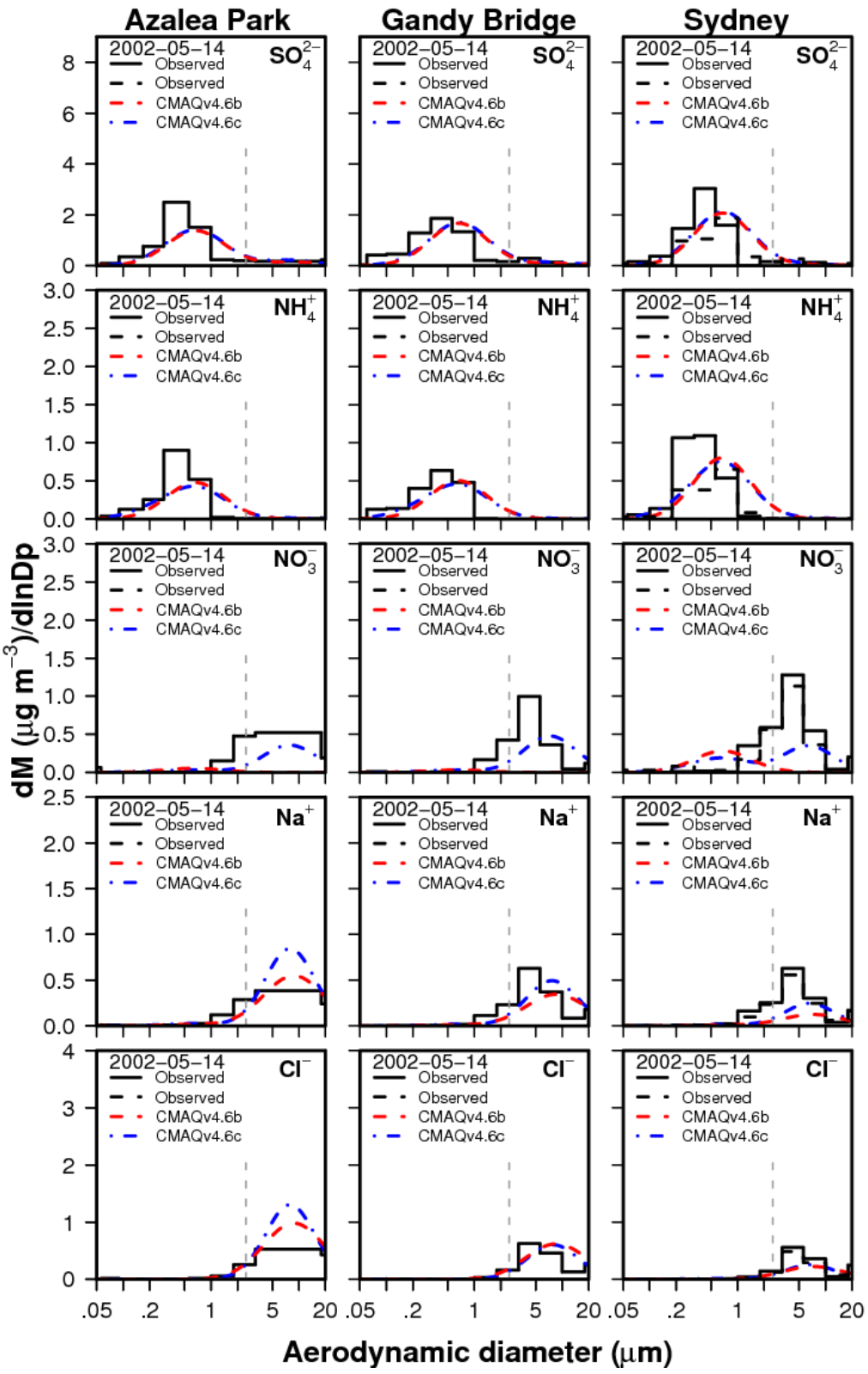

Fig. S5. Observed and predicted size distributions of inorganic particle components at three Tampa-area sites averaged over a 23-h period on 14 May 2002.

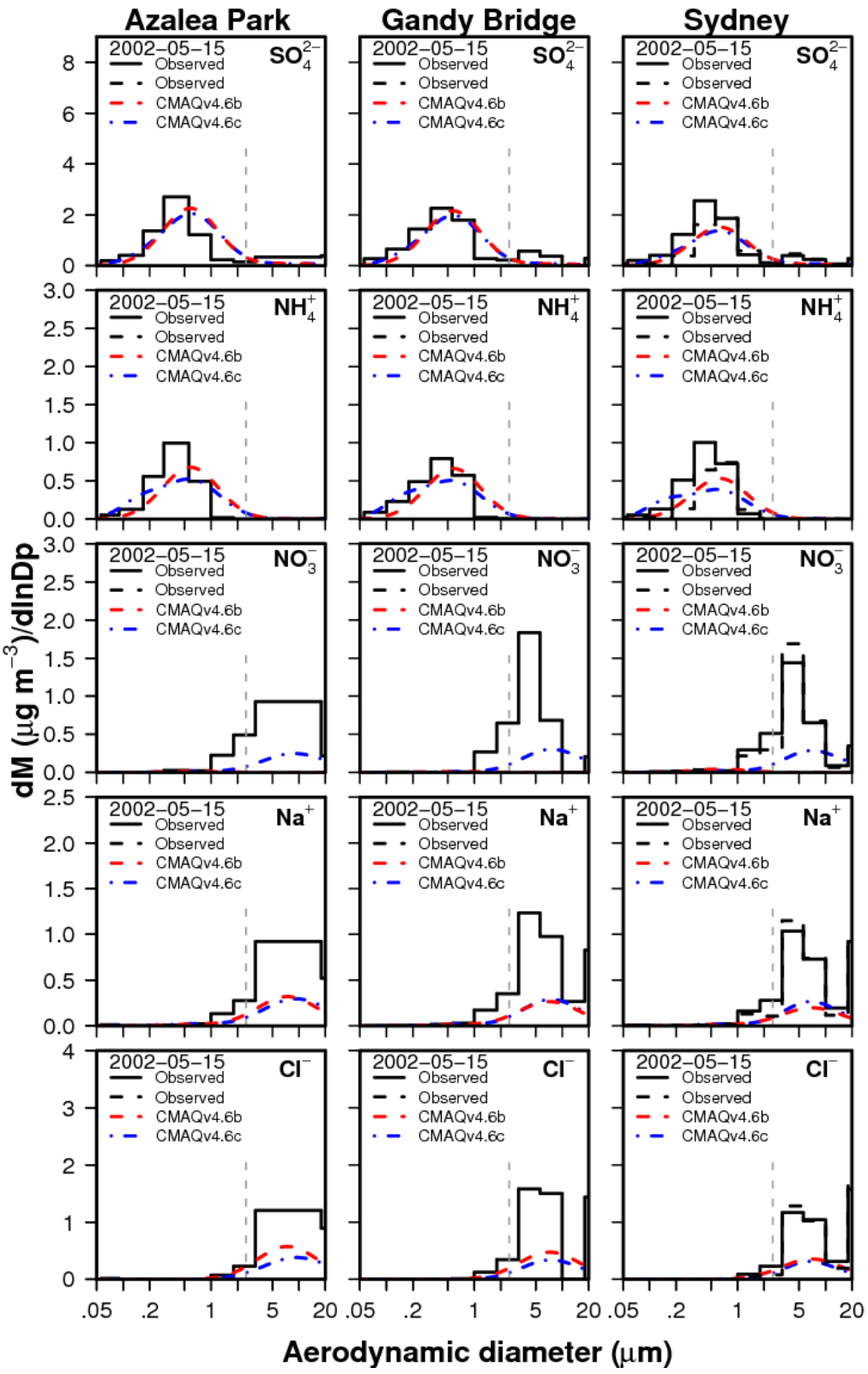

Fig. S6. Observed and predicted size distributions of inorganic particle components at three Tampa-area sites averaged over a 23-h period on 15 May 2002.

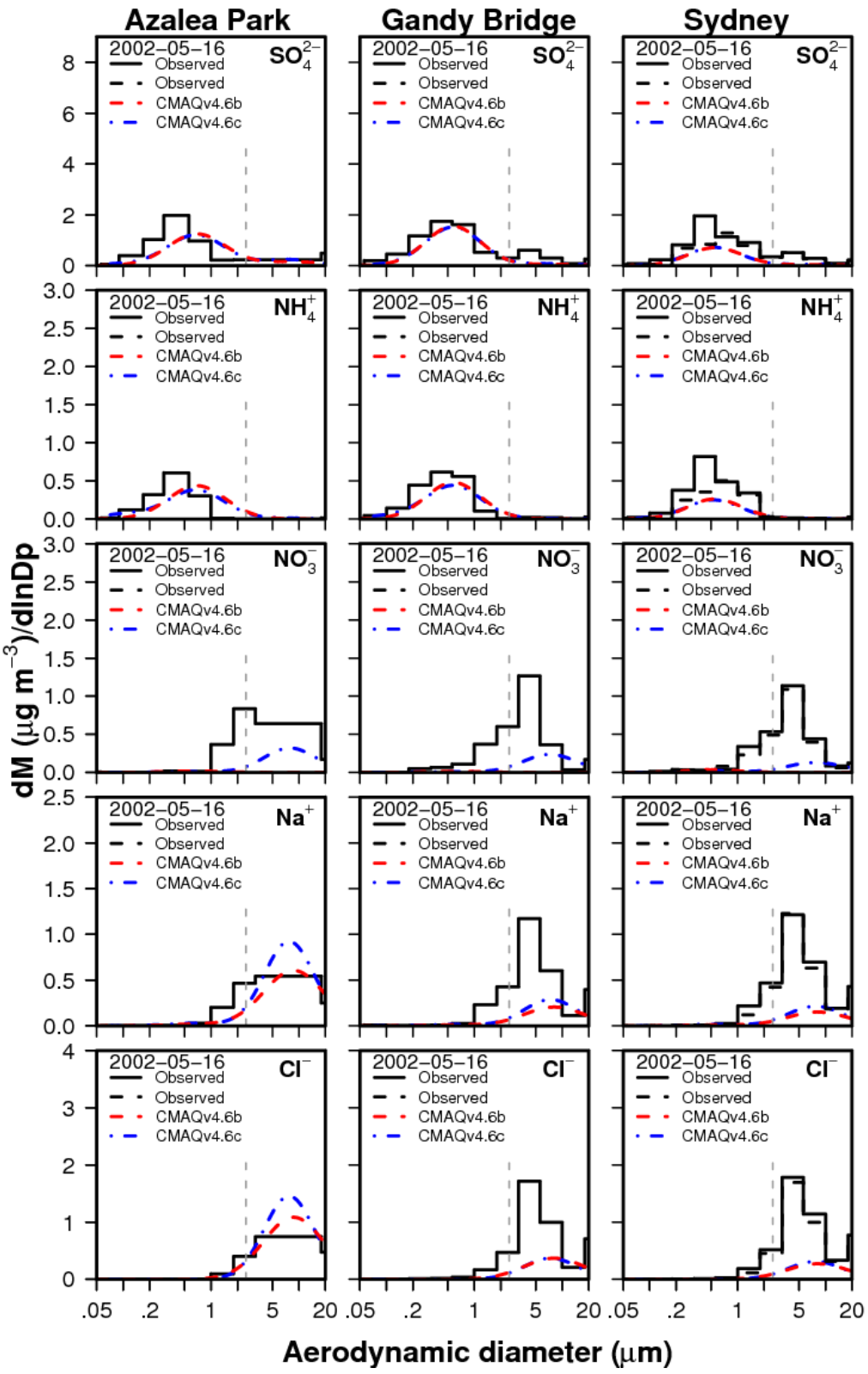

Fig. S7. Observed and predicted size distributions of inorganic particle components at three Tampa-area sites averaged over a 23-h period on 16 May 2002.

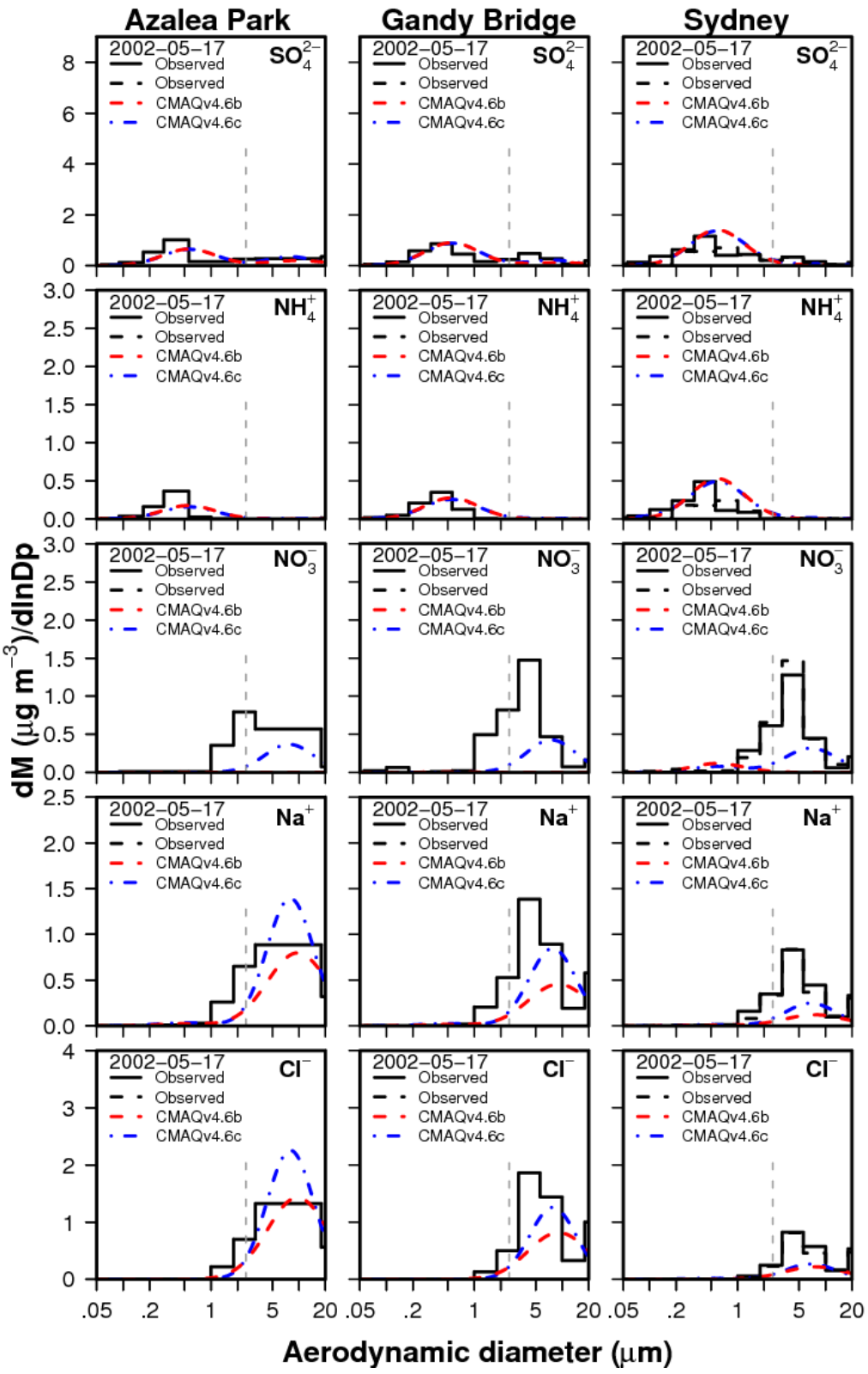

Fig. S8. Observed and predicted size distributions of inorganic particle components at three Tampa-area sites averaged over a 23-h period on 17 May 2002.

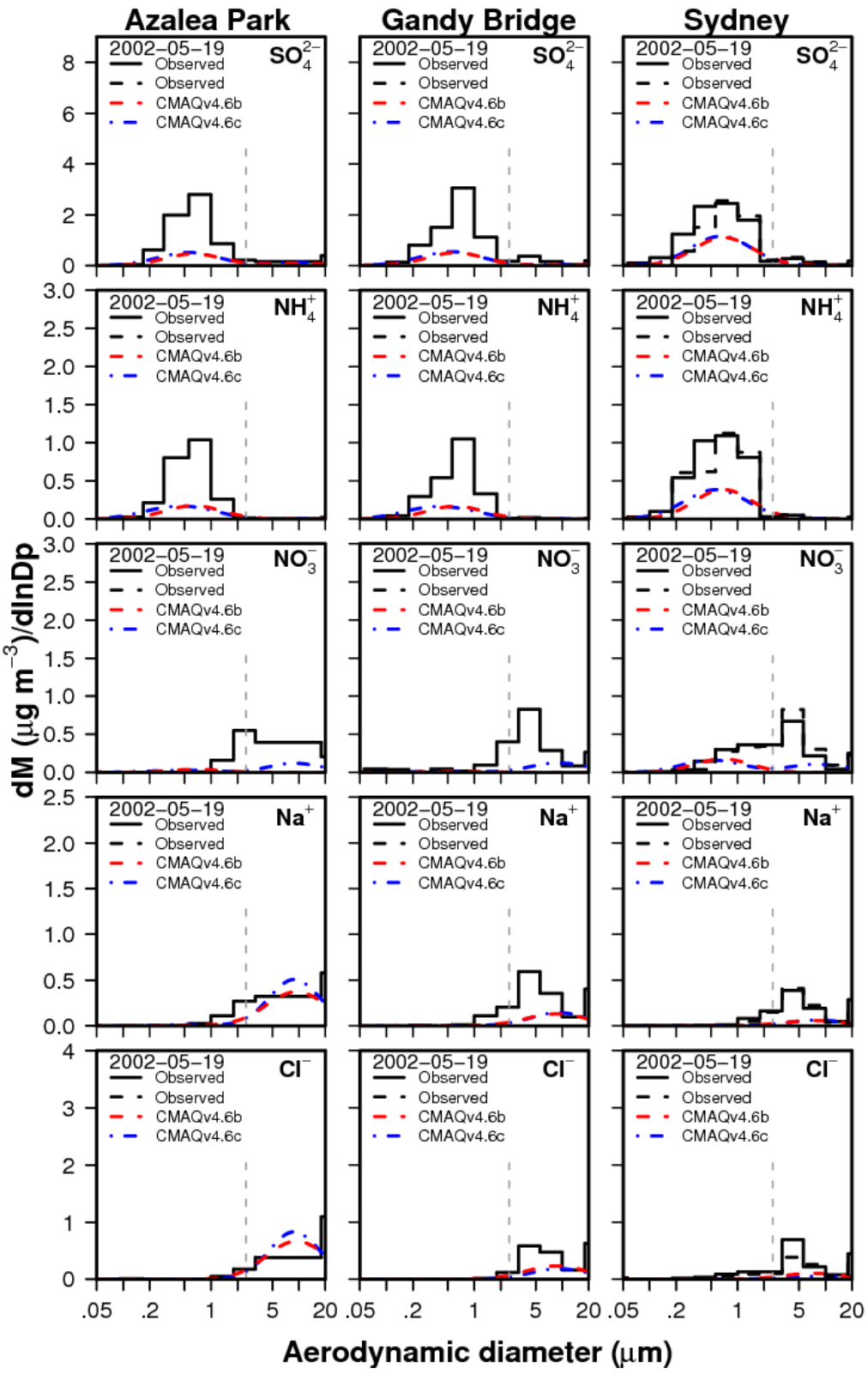

Fig. S9. Observed and predicted size distributions of inorganic particle components at three Tampa-area sites averaged over a 23-h period on 19 May 2002.

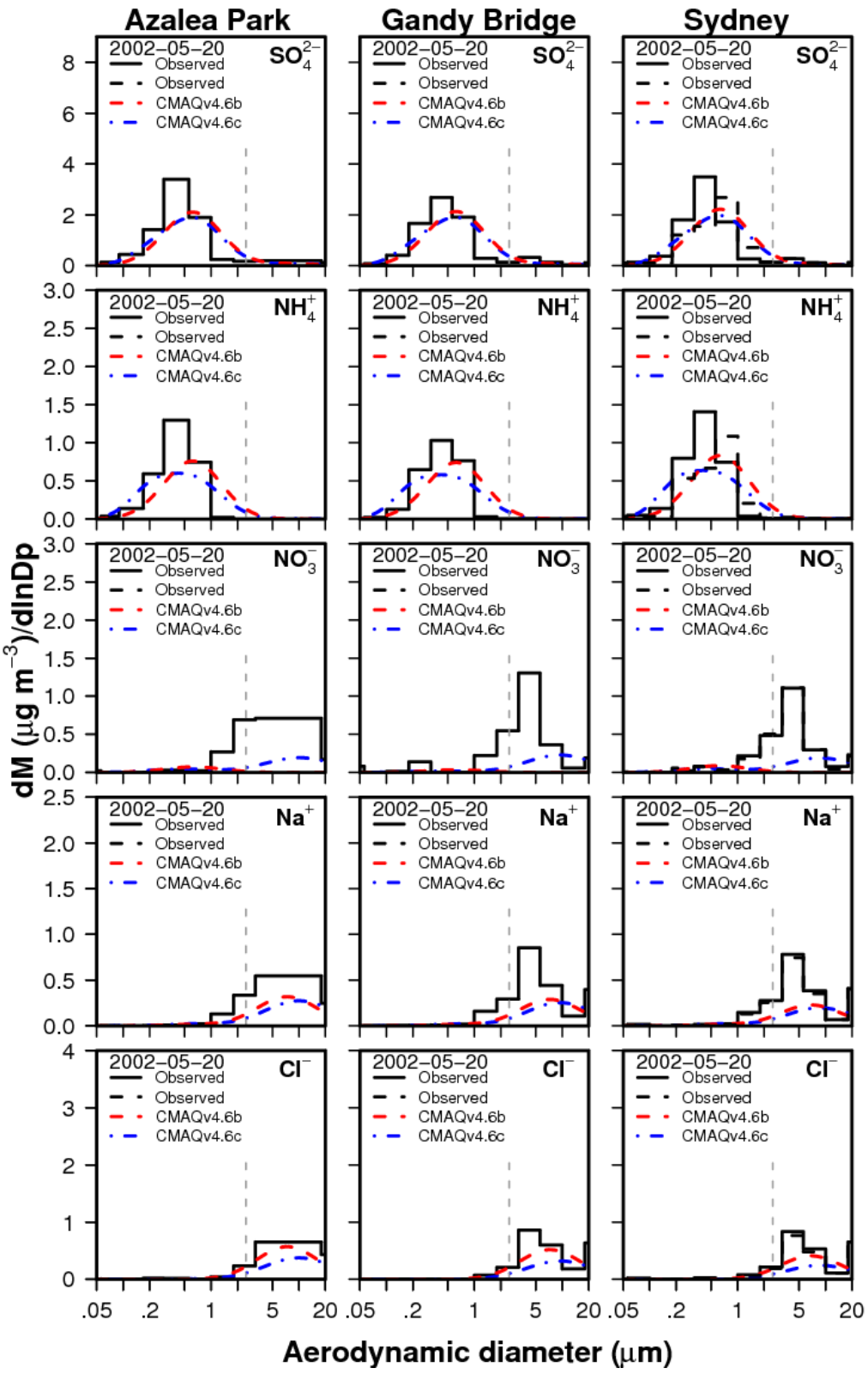

Fig. S10. Observed and predicted size distributions of inorganic particle components at three Tampa-area sites averaged over a 23-h period on 20 May 2002.

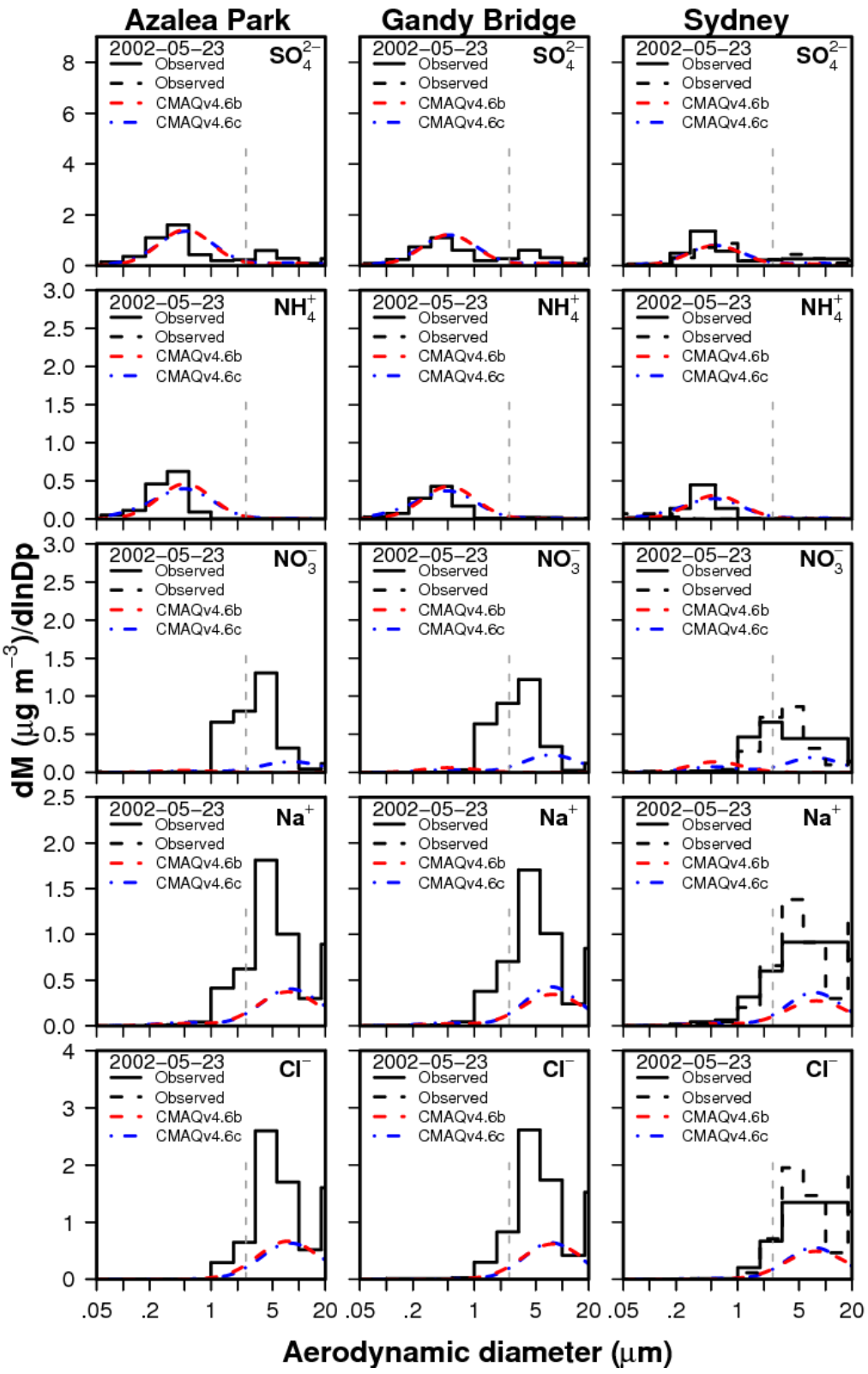

Fig. S11. Observed and predicted size distributions of inorganic particle components at three Tampa-area sites averaged over a 23-h period on 23 May 2002.

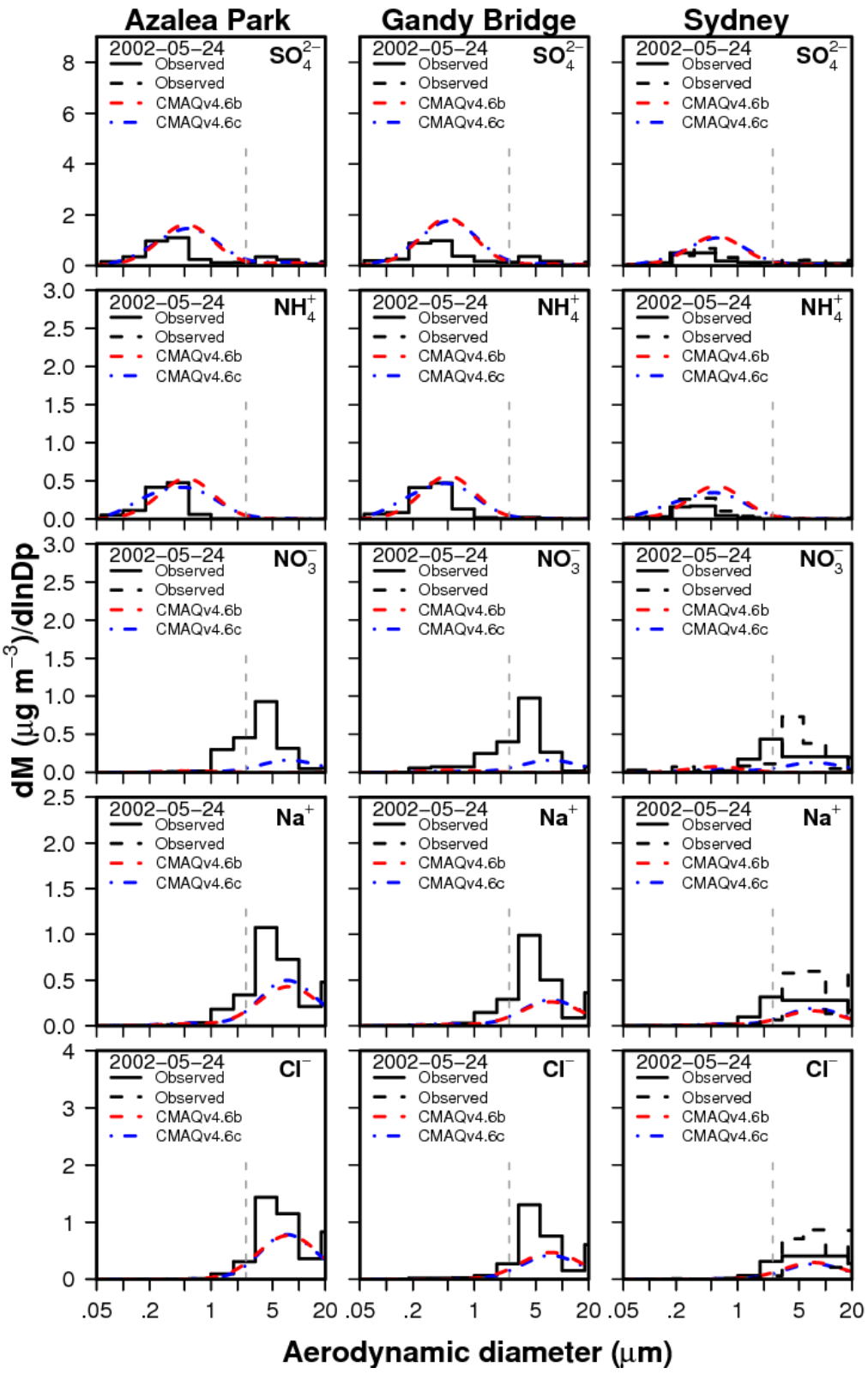

Fig. S12. Observed and predicted size distributions of inorganic particle components at three Tampa-area sites averaged over a 23-h period on 24 May 2002.

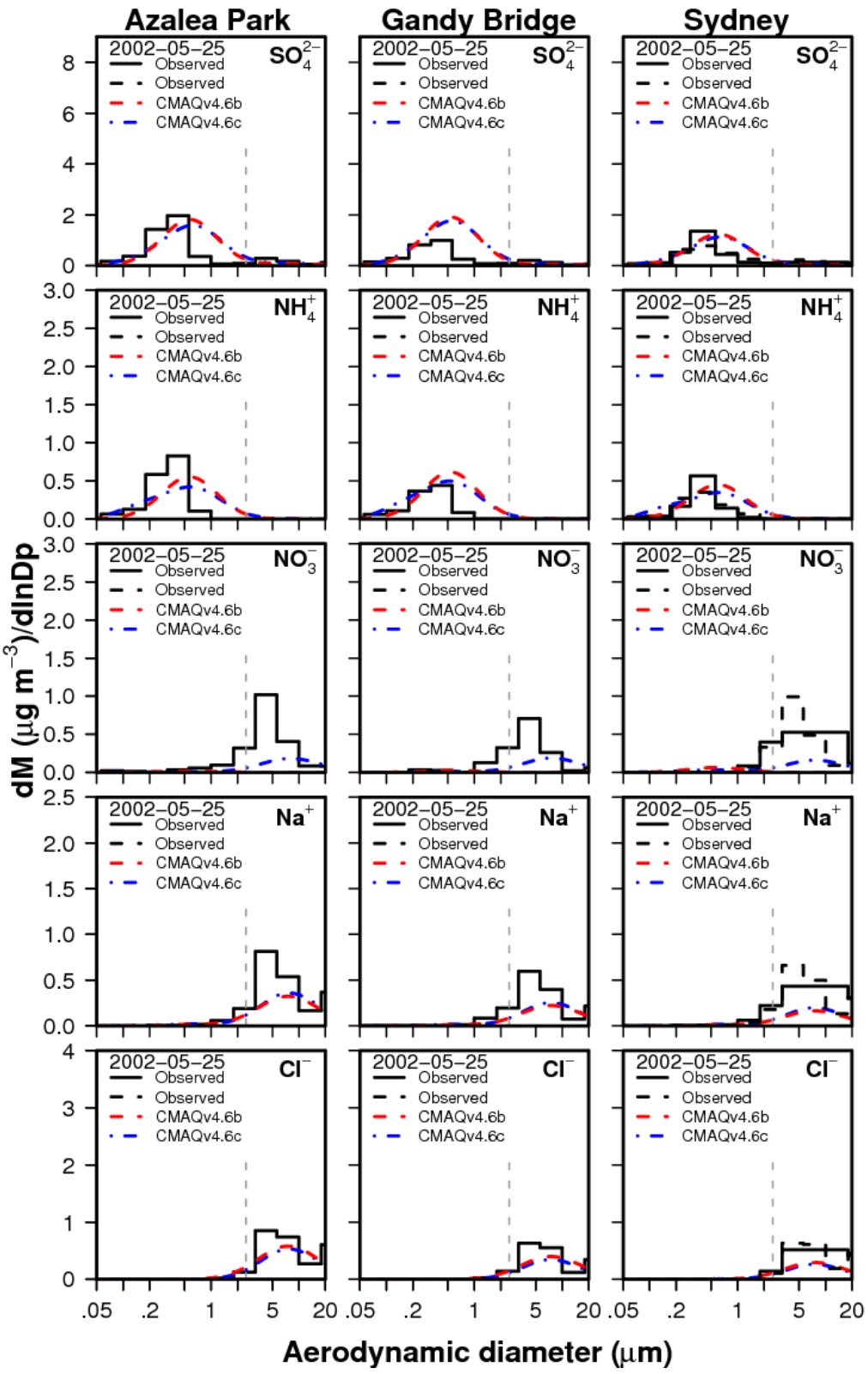

Fig. S13. Observed and predicted size distributions of inorganic particle components at three Tampa-area sites averaged over a 23-h period on 25 May 2002.

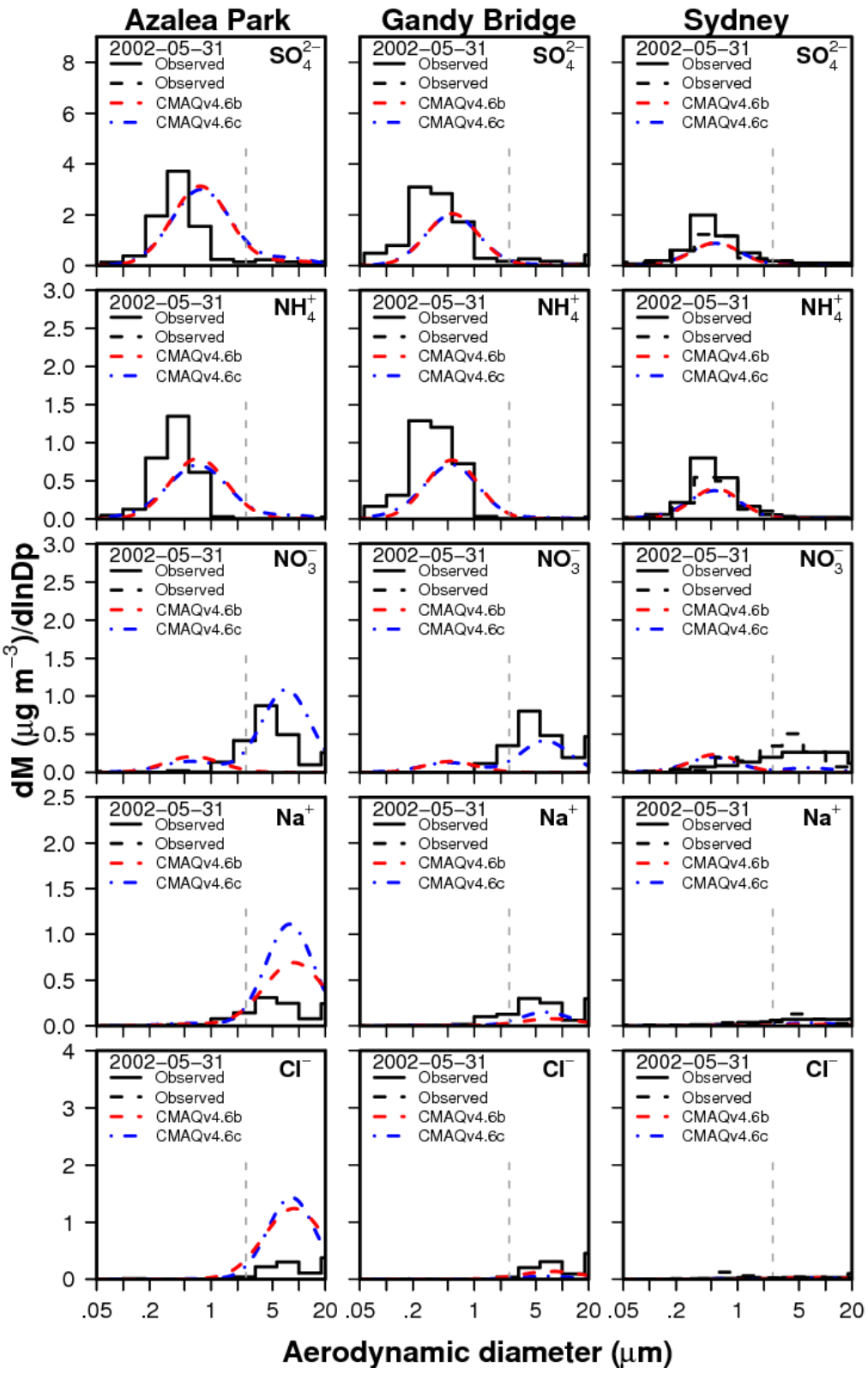

Fig. S14. Observed and predicted size distributions of inorganic particle components at three Tampa-area sites averaged over a 23-h period on 31 May 2002.

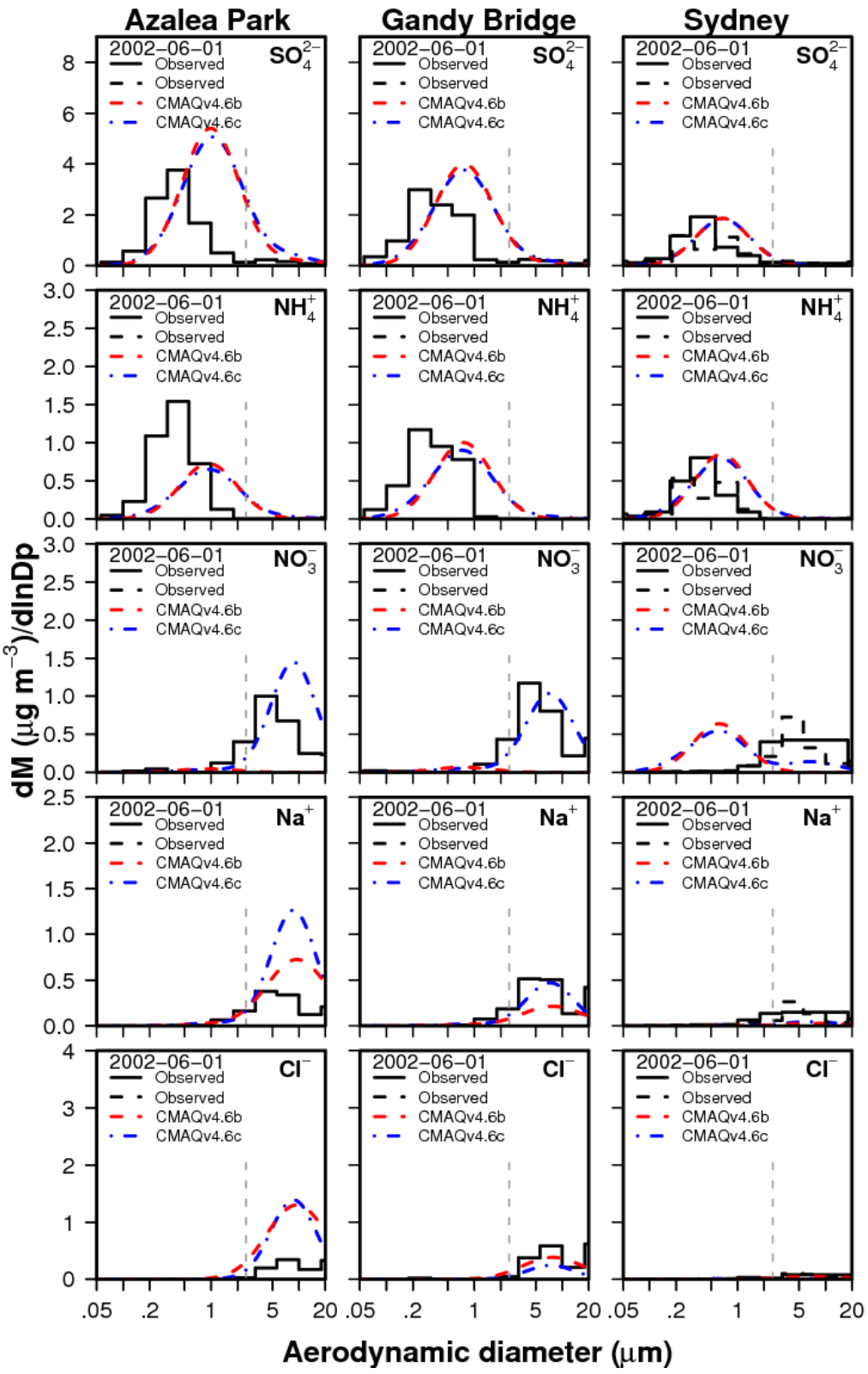

Fig. S15. Observed and predicted size distributions of inorganic particle components at three Tampa-area sites averaged over a 23-h period on 1 June 2002.

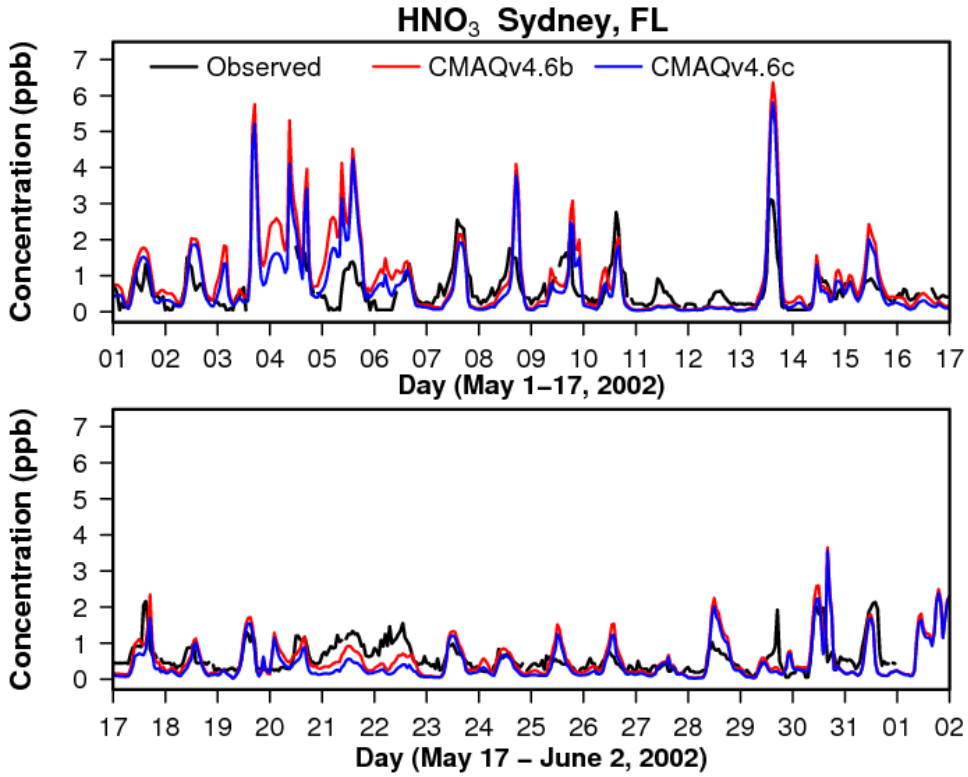

Fig. S16. Time series of observed and modeled nitric acid concentration at the Sydney, FL site from 1 May – 2 June 2002. Tick marks represent 0000 local standard time on each day.

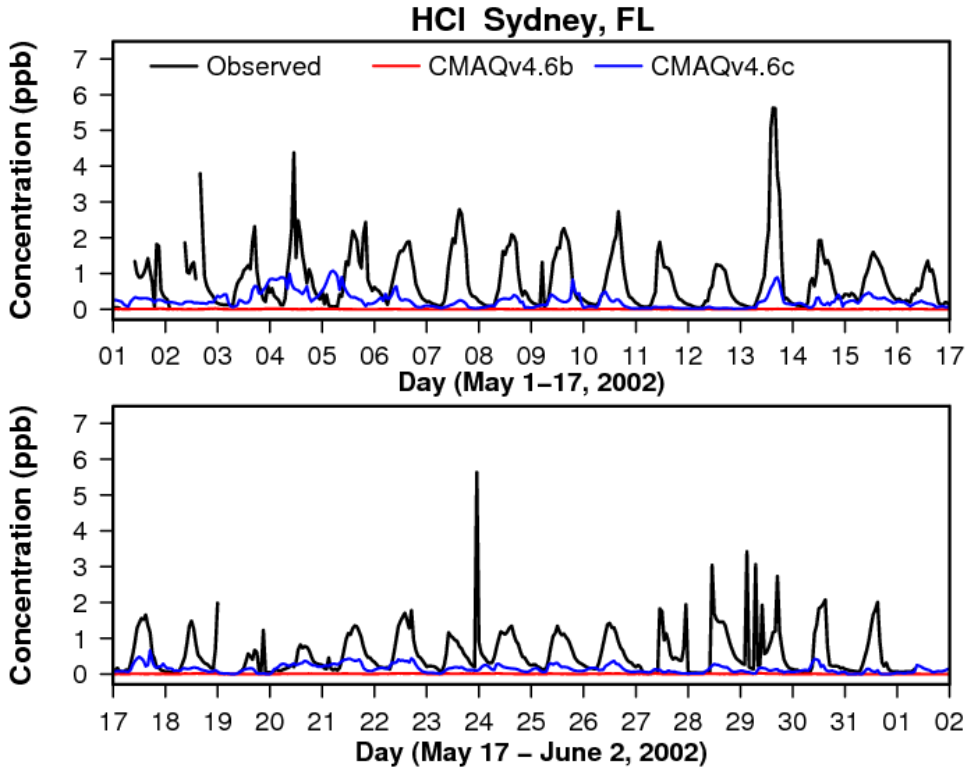

Fig. S17. Time series of observed and modeled hydrochloric acid concentration at the Sydney, FL site from 1 May – 2 June 2002. Tick marks represent 0000 local standard time on each day.

Open-Ocean and Surf-Zone Grid-Cell Allocation

In CMAQ, sea-salt emissions are calculated using a gridded file (i.e., OCEAN_1 file) that contains values for the fraction of each cell classified as open-ocean and coastal surf zone. The OCEAN_1 file created for our domain is based on shoreline data of the NOAA Office of Coastal Survey (i.e., the U.S. Seamless Merged Mean High Water Vector Shoreline data). These shoreline data were processed into a shapefile and imported into Geographic Information System (GIS) software (ArcInfo, www.esri.com). A 250-m tolerance was used in ArcInfo to remove vertices and smooth arcs in the shapefile and to ensure acceptable surf-zone classification in areas with complex shorelines. Shoreline arcs were classified as surf-zone or non-surf-zone based on the local coastal features. The shoreline of the bay near the Gandy Bridge site was classified non-surf zone, as were other bays, river inlets, and shorelines protected by barrier islands. The Spatial Allocator tool (documentation and code for the Spatial Allocator are available from http://www.cmascenter.org/) was used to convert data from the GIS-based shapefile into the gridded OCEAN_1 file used in the CMAQ simulations. Instructions on using the Spatial Allocator to compute the grid-cell fraction covered by land, open-ocean, and coastal surf zone are available in Section 7.1.6 of the following: http://www.ie.unc.edu/cempd/projects/mims/spatial/alloc.html. The surf-zone fraction of a grid cell was computed here assuming a 50-m-wide surf zone adjacent to shoreline arcs with a surf-zone classification.

Additional Details on Coarse Particle Modeling in CMAQv4.7 (from Release Notes)

In previous versions of CMAQ, coarse-mode particles were assumed to be dry and inert, and components in the coarse mode could not evaporate or condense. This approach does not allow important aerosol processes, such as replacement of chloride by nitrate in mixed marine/urban air masses, to be simulated. In CMAQ v4.7, the code has been updated to allow semi-volatile aerosol components to condense and evaporate from the coarse mode and nonvolatile sulfate to condense on the coarse mode. Since coarse-particle components are often not in equilibrium with the gas phase, dynamic mass transfer is simulated for the coarse mode (whereas the fine modes are equilibrated instantaneously with the gas phase). This treatment can be found in the new VOLINORG subroutine, which is embedded in the aero_subs.f subprogram.

In coastal regions, significant emissions of sea salt originate from wave-breaking in the surf zone. Previous versions of CMAQ did not account for this process. In CMAQ v4.7, surf-zone emissions are computed in the ssemis.F subprogram by assuming that the surf zone is covered entirely by whitecaps (i.e., WCAP = 1) and that the size distribution of sea salt emitted from the surf zone is identical to that emitted from the open ocean.

The computational efficiency of the CMAQ aerosol module is governed largely by the number of calls to ISORROPIA. In previous versions of CMAQ, only one ISORROPIA call per model time step was required to equilibrate the fine-particle composition with the gas phase. In CMAQ v4.7, additional ISORROPIA calls are required during each time step to transfer inorganic gases to and from the coarse mode. In an effort to preserve computational efficiency, coarse-mode mass transfer is skipped when either RH < 18% (i.e., the metastable aerosol assumption is questionable) or the summed concentration of coarse NH4, SO4, NO3, and Cl is less than 0.05 ug/m3 (i.e., coarse-mode mass transfer is of negligible importance). Alternatively, users may turn off the coarse-mode mass transfer altogether by setting HYBRID = .FALSE. in the VOLINORG subroutine (line 2827 of aero_subs.f). This is only recommended for model sensitivity studies or for applications in which the inorganic PM composition is of less importance than minimizing model runtime.

In previous versions of CMAQ, ISORROPIA was always run in the 'forward' mode, which partitions total-system concentrations between the gas and particle phases. In CMAQ v4.7, the 'reverse' mode of ISORROPIA is used for the first time. In this mode, vapor pressures of the gas-phase components are predicted based on the particle-phase composition, temperature, and RH. These vapor pressures are needed to determine the chemical driving potential between the gas phase and the coarse-particle mode. During testing, we found that ISORROPIA in reverse-mode occasionally returns negative vapor pressures [i.e., variables GAS(1), GAS(2), and/or GAS(3) are less than zero]. A corrected version of ISORROPIA was not available in time for this CMAQ release so, as an interim measure, volatile inorganic species are not transferred to/from the coarse mode during the integration time steps when negative vapor pressures are returned by ISORROPIA and a descriptive warning is written to the log file.

In previous versions of CMAQ, the standard deviation of the coarse-mode particle size distribution was fixed at 2.2, and sulfate was the only condensing component to influence fine-mode standard deviations. In CMAQ v4.7, the standard deviations of all three modes are variable. However, a constraint is imposed such that standard deviations of the accumulation and coarse modes cannot change during the condensation process (see LIMIT_Sg in the GETPAR subroutine, which is contained in the AERO_INFO.f subprogram). This is a temporary patch that was required to achieve a numerically stable solution during dynamic mass transfer, and we hope to relax this constraint in a future public release of CMAQ.

In conjunction with the updated coarse-mode treatment, two new species were added to AE_SPC.EXT: ANH4K and SRFCOR. ANH4K represents the coarse-mode ammonium ion and SRFCOR represents the surface area of coarse-mode particles. All of the AE5 mechanism include files in CMAQv4.7 include these new species. Coarse-mode water (AH2OK) and nitrate (ANO3K) were included in the AE4 mechanism files released with previous versions of CMAQ, but their concentrations were fixed at zero. In the AE5 module, these concentrations are nonzero. The default boundary concentration profile does not include species commonly associated with sea-salt (e.g., ANAJ, ACLJ, ANAK, ACLK, ASO4K, ANO3K, etc.). For model applications in which one or more of the domain boundaries lies over the ocean, users are urged to add these species to the boundary profile.